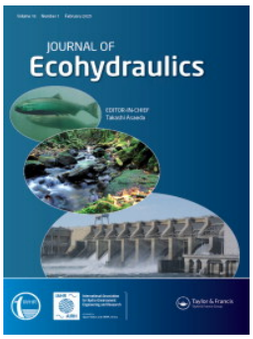

Journal of Ecohydraulics

ISSN: (Print) (Online) Journal homepage: www.tandfonline.com/journals/tjoe20

Morphodynamics of ecological scours as deep pool habitats

Christin Kannen, Frank Seidel & Mário J. Franca

To cite this article: Christin Kannen, Frank Seidel & Mário J. Franca (24 Jan 2025): Morphodynamics of ecological scours as deep pool habitats, Journal of Ecohydraulics, DOI: 10.1080/24705357.2024.2426808

To link to this article: https://doi.org/10.1080/24705357.2024.2426808

JOURNAL OF ECOHYDRAULICS
https://doi.org/10.1080/24705357.2024.2426808

Morphodynamics of ecological scours as deep pool habitats

Christin Kannen, Frank Seidel and Mário J. Franca

Institute for Water and Environment, Karlsruhe Institute of Technology, Karlsruhe, Germany

ABSTRACT

Climate change leads among other consequences to extreme hot and dry periods in summer with extremely low water depths which impose an increasing threat to fish populations in river systems. For example, in south-western Germany severe fish mortality was observed in the extreme summer of 2018 which could be justified by a lack of deep pool habitats providing enough water depth and cold-water refuges. This study aims to provide engineering measures to create local scours that should fulfil the function of sustainable deep pool habitats. In this research, six different prototypes common in-stream measures are tested experimentally under clear-water scour conditions, to quantify their ability to create local scours and based on that to evaluate habitat suitability as deep pool habitats but also to asses potential increase of flood risk in the areas of intervention. The results show that all investigated measures were able to meet the target values of the necessary water depth and area requirements recommended from fish biological studies. The backwater rise and associated increase of flood risk due to the in-stream measures were also quantified showing that these need to be considered in the planning of river restoration projects.

ARTICLE HISTORY
Received 19 June 2023
Revised 23 September 2024
Accepted 6 October 2024

KEYWORDS
Hydromorphology; nature-based solution; movable bed experiments; backwater rise; ecomorphology; flood risk; in-stream structures; river revitalization

1. Introduction

Due to human activities such as rectifications and channelizations, river systems have lost large parts of their hydromorphological quality (Wohl 2019). Furthermore, one of the observed effects of global warming in central European river systems is a reduction in available water in dry periods, in many cases reaching the level of droughts. Low water levels in combination with a lack of hydromorphological diversity in rivers and consequently no sufficient water depth during low water periods, leads to an increasing threat to fish biocenosis. The reduction of suitable habitats during drought season also can lead to a concentration effect and consequently to an increased density of fish (Magoulick and Kobza 2003). Hence, river managers ask for measures to increase resilience of river ecosystems in face of extreme low water periods. Missing habitat diversity, especially deep pool habitats, was detected to be one of the main problems of the Southern German river systems. Deep pool habitats are a key habitat during drought seasons due to large water depth and surface area. Deep pool habitats provide several functions besides sufficient water depth during summer such as flow-shelter outside the main flow path during flood events, and refuge during wintering season in connection with suitable structures and visual shelter as protection from predator birds such as cormorant (Magoulick and Kobza 2003). So, deep pool habitats are multifunctional aquatic structures with a vital importance for fish populations.

In this study, different engineering measures to create scour holes and their ecological potential for fish habitat are investigated. The selection and conceptualization of these measures are based on a cross-literature review in the areas of hydromorphology and fish biology. The research showed that in-stream measures are widely applied methods in revitalization projects with the aim of diversifying river bed morphology, water depth and flow velocities. Previous studies have looked at one type of structure at a time, e.g. micro groynes (Mende 2014; Müller et al. 2020), and investigated their effect on bed morphology and flow velocities. Possible habitat types are then derived from the respective induced changes. In this study, the focus is on the intended use of structures for the creation of a specific habitat type instead of looking at one specific structure type and the resulting habitat types. Therefore, different types of in-stream structures are tested and compared, regarding their ability to create local scouring, under the same boundary conditions.

CONTACT Christin Kannen Christin.Kannen@kit.edu Institute for Water and Environment, Karlsruhe Institute of Technology, Karlsruhe, Germany

Formerly, a strong focus in scouring research was on the prediction of maximum scour depth in the vicinity of engineering infrastructures such as bridge piers (Akhlaghi et al. 2020; Chiew and Melville 1987; B. Melville 2008; Raudkivi 1986; Raudkivi and Ettema 1983), abutments (Coleman et al. 2003) and downstream of weirs and gates (Guan et al. 2014). Later, local scouring was also investigated close to river training structures in navigation channels, such as groynes and groyne fields (Anlauf and Hentschel 2007; Hentschel et al. 2012). In all cases, an attempt was made to reduce the scour depth by means of rip rap structures or river bed and bank protection measures. In the engineering community, the linkage of obstacle-induced scour holes and their potential use as habitats was made by Kurdistani (2013) and Pagliara et al. (2013, 2014, 2015) who implemented in-stream structures such as cross vanes for the creation of ecological scours. In freshwater ecology naturally occurring scours e.g. in riffle-pool-sequences have been studied since decades (Thompson 2018). For obstacle-induced scour, ecology uses the term "forced pools".

The habitat suitability analysis in this study is limited to the species *Barbus Barbus*. Due to specific habitat needs during their life stages and different daily and seasonal preferences, the barbel is a good indicator for structural diversity of rivers (Britton and Pegg 2011). The deep pool, which is investigated in this study, is preferred by the adult barbel as resting area during daytime and as winter habitat (LAVES (Hrsg.)) 2011). Further specifications on the deep pool habitat are rare in literature (Melcher and Schmutz 2010; Peñáz et al. 2002). Preferred water depths are given with larger than 1 m (Blohm et al. 1994), 2–6 m (Bănărescu and Bogutskaya 2003), $0.6-2.0$ m (Pouilly and Souchon 1994) and $0.5-1.8$ m (Peñáz et al. 2002). In regulated rivers of first order a mean water depth of 4.2 m with a range of 2.5–8 m was detected (Panchan et al. 2022) even though the authors mention that it remains an open question whether this habitat preference would correspond equally to an unregulated river.

As the research focuses on river systems in southern Germany the qualitative habitat specifications given in the directive Landesstudie Gewässerökologie (LSGÖ) (A. Becker and Ortlepp 2022) were taken as target values. The LSGÖ characterizes habitat types according to physical parameters such as water depth, mean flow velocity at the surface and sediment size. Further necessary functions, such as shelters, are described qualitatively. Within this guideline, a deep pool habitat for a barbel is characterized by a water depth of greater than 2 m on an area of at least 6 m^2, and a flow velocity preferably between 0.3 and 0.6 m/s. The qualitative values correspond well with literature values from France, Belgium and Czec Republic as mentioned above and seem to represent a deep pool habitat for a barbel in a sufficient accuracy for hydromorphological engineering design. For the evaluation of habitat suitability water depth and velocity are equally important. This publication focuses on the target water depth, velocity data were also measured but will be published elsewhere.

Implementing an in-stream structure into a river cross-section increases the blocked area and leads to an increase of the flow resistance. The energy loss is compensated by a rise of the upstream water level, which might be in conflict with flood protection issues. In particular, the engineering structures presented in this work are focusing on urbanized areas where other measures than in-stream structures are not possible to implement due to side restrictions. In urbanized areas, the water surface elevation often is of sensitive nature, as the backwater rise of in-stream structures must not lead to an overtopping of flood protection measures such as levees.

Moreover, most studies on clear-water scouring focus only on one structure type such as emergent piers (B. Melville 2008), abutments (B. Melville 1997) or submerged structures vanes (Pagliara et al. 2013, 2014, 2015; Pagliara and Kurdistani 2013). Thus, it is very difficult to cross-compare different studies e.g. from pier vs. abutment scour. As we investigate different engineering structures but for the same flow and sediment conditions we yield towards a direct comparability of scour shape and size.

The objective of the study is to compare six different in-stream measures regarding their ability to locally changing the river morphology providing a deep pool habitat on the basis of their respective scour pattern. A second derived objective is the evaluation of the effect of these in-stream measures on backwater rise, for a better assessment of the flood risk when implementing these. Most investigations focus either on habitat suitability or flood management of in-stream structures. This study aims to provide the data basis for both, the scour pattern for the evaluation of structural morphological diversity and its ecological benefits but also looking at the effects of flood risk of the different in-stream structures.

2. Morphologic and hydraulic effects of prototype in-stream measures

The structures investigated within this study are divided into three groups according to their interference with the channel flow (flow type). Pier-like structures are emergent ($h_s > h_0$) and are flown around laterally on both sides ($w_s < w$), stone-like structures are submerged ($h_s < h_0$) and are flown laterally on both sides and are overflown ($w_s < w$) and dam-like structures are submerged ($h_s < h_0$)

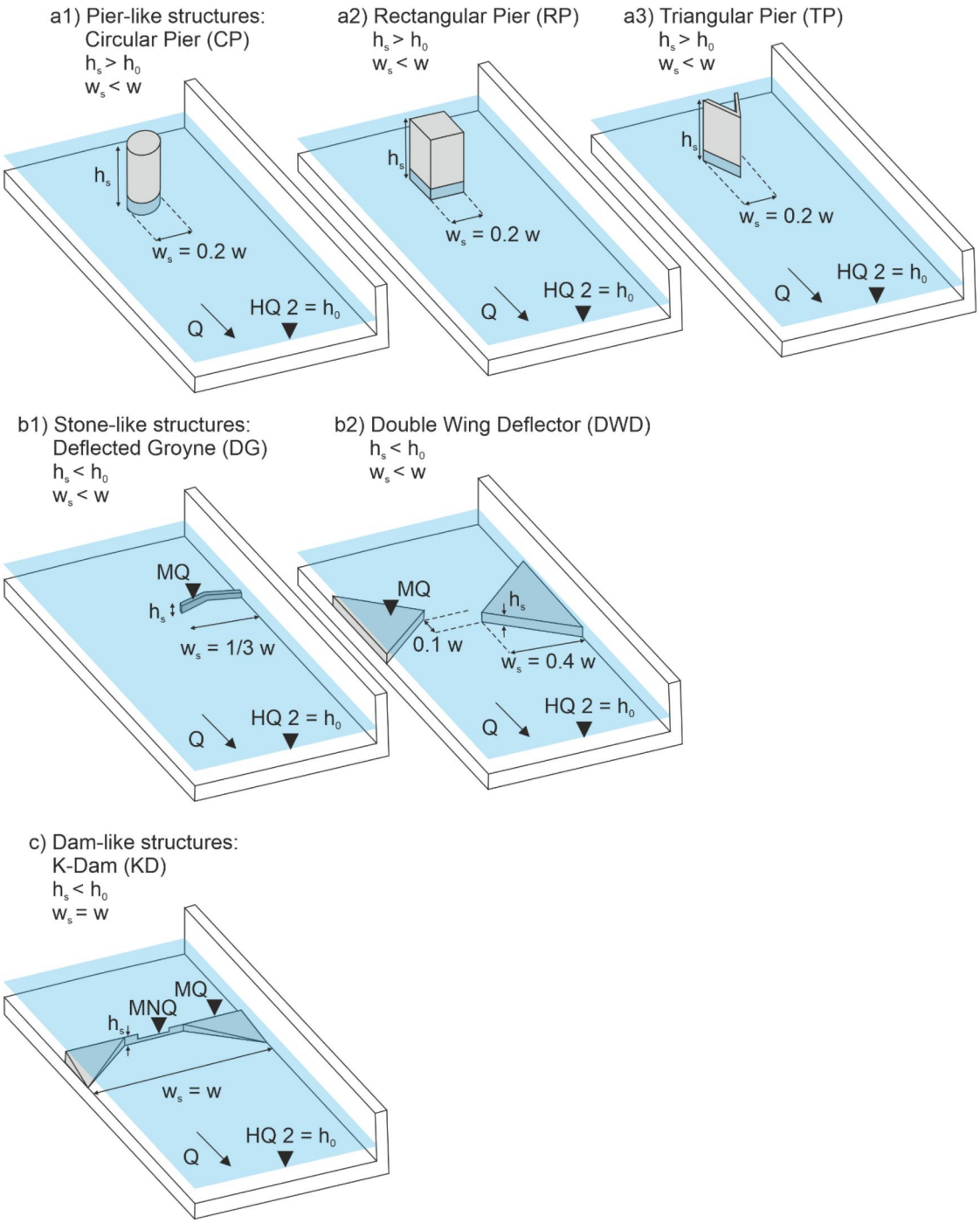

Figure 1. Overview of different in-stream structures herein tested and corresponding flow types and scouring processes. (a) Pier-like structures: Circular pier (CP), Rectangular pier (RP) and Triangular pier (TP), (b) stone-like structures: Deflected groyne (DG), Double Wing Deflector (DWD) and (c) dam-like structures: Kdam (Kdam).

and cover the whole river width ($w_s = w$) and are overflown (see Figure 1).

For the basic comprehension of scour processes around different structures an overview of the flow field and the resulting bed morphology as reported in literature is essential.

2.1. Pier-like structures

The complex flow patterns around a cylindrical pier are well known (see e.g. Breusers and Raudkivi 1991). At the upstream side of the pier a backwards rotating surface roller forms and a strong downflow immediately upstream of the cylinder is induced. The velocities in the downflow can reach a maximum of 0.6–0.8 U_0 (Dey and Raikar 2007; Raudkivi 1986). The downflow acts like a vertical jet and erodes sediment upstream of the cylinder (Akhlaghi et al. 2020). This is the starting point of the horseshoe vortex which is the main driver of the scour process. Downstream of the cylinder a wake vortices system with backwards rotating whirls and a dead water zone forms due to

alternating separations of the flow on both sides of the cylinder (Akhlaghi et al. 2020; Breusers et al. 1977).

Due to this vortex system a complex bed morphology is formed. The relevant parameters of scour formation and scour depth can be divided into the groups of flow parameters (ρ, ν, g, flow intensity U_o/U_c, relative flow depth h_0/D), sediment parameters (ρ_s, σ_g, relative sediment size D/d_{50}) and geometrical parameters of the structure (relative width D/w, alignment and shape of pier) (Akhlaghi et al. 2020; B. Melville 2008; Raudkivi 1986). The scour pattern around pier-like structures such as cylindrical and rectangular piers were investigated in several works (Dey and Raikar 2007; Khosronejad et al. 2012). The circular (CP) and rectangular pier (RP) both develop the deepest part of the scour immediately upstream of the structure and the scour hole spreads radially with decreasing depth which is attributed to the turbulent horseshoe vortex system. The maximum relative scour depth is $d_s/D = 1.3$ for Dey and Raikar (2007) and -0.36 for Khosronejad et al. (2012). Downstream of the structure a significant dune can be observed with a distance of $l_{dune} = 6.7\,D$ for Dey and Raikar (2007).

To the authors knowledge the influence of triangular piers on the flow field and bed morphology has not been investigated systematically yet.

2.2. Stone-like structures

In comparison with pier-like structures, stone-like structures are submerged. The effect of submergence on the flow field and scour process was systematically studied e.g. by Dey et al. (2008), Ishigaki and Baba (2004) and Shamloo (1997). The dominating parameter on the scouring process are the same as for pier-like structures with additional parameters for (I) groynes such as relative submergence h_s/h_0, shape of the structure, angle of attack, length of the groyne, tailwater depth h_2 and position in the river cross section (Armanini et al. 2010; Breusers and Raudkivi 1991; Ishigaki and Baba 2004; Möws and Koll 2014; Pagliara et al. 2013, 2015) and (II) bluff bodies (boulders) such as obstacle Reynolds number, blockage ratio including obstacle height and width as well as projected frontal area (Euler et al. 2017; Euler and Herget 2012), the volume of the boulder (Fisher and Klingeman 1984) and the width of the structure (hemisphere (Shamloo 1997) and cube (Huang 1991)).

Groynes are investigated widely in the use case of water level management in navigation channels, but it has been detected that they also cause scouring especially at the head of the groyne (Anlauf and Hentschel 2007; Hentschel et al. 2012). Ishigaki and Baba (2004) studied the influence of different submergence ratios for groynes in flume experiments. The maximum scour depth occurs at the head of the groyne and increases with decreasing submergence ratio reaching a maximum for the unsubmerged case. Harada et al. (2013) characterized the influence of the angle of attack on submerged groynes. A 90° angle towards the flow caused the deepest and shortest scour hole. With increasing angle of attack (with constant blockage ratio and therefore increasing length of the groyne) decreasing scour depth and increasing length of the scour hole could be detected.

Boulders as simple habitat structures, idealized in forms of hemispheres, cubes, natural rocks and submerged cylinders were investigated by Shamloo (1997), Burkow and Griebel (2016), Dey et al. (2008) and Euler and Herget (2012), Euler et al. 2017). Four different flow regimes are distinguished. Regime 1 to 3 ($h_0/h_s = 1.1$ to > 4) are surface flow regimes where a jet stays at the surface even downstream of the obstacle. For $h_0/h_s < 1$ the regime 4 is an impinging jet regime.

Submerged circular piers were investigated by Dey et al. (2008) and Euler and Herget (2012), Euler et al. (2017). Downstream of the obstacle an arch vortex, hairpin vortices and trailing vortices develop due to the overflow above the submerged structure. The wake region extends up to four obstacle diameters into downstream direction and shows a current in upward direction. Further research showed that the same flow patterns can not only be observed for submerged cylinders but also for cobbles (Euler et al. 2017) and cubes (Burkow and Griebel 2016).

Upstream of the primary horseshoe vortex is a smaller, less coherent secondary horseshoe vortex cell (Kirkil et al. 2008). A step forms inside of the scour hole with gradually changing slopes in front of the obstacle from less steep to a steeper slope (Euler et al. 2017; Euler and Herget 2012). Within the two-step system two horseshoe vortex cells form which are the reason for the step to evolve (Kirkil et al. 2008). With increasing submergence, the dimension and strength of the horseshoe vortex decreases and results in a decrease in scour depth (Dey et al. 2008).

2.3. Dam-like structures

The flow field of a dam-like structure was described in detail by Guan et al. (2014) and Wu and Rajaratnam (1996) who performed laboratory experiments with sharp crested fully submerged dams in a rectangular flume. According to their findings, the flow regimes can be classified as surface-flow regimes (regimes 1–3) and impinging jet

regime (regime 4) (Wu and Rajaratnam 1996). The flow regimes are dependent on the water level differences upstream and downstream of the dam and the approach flow rate (Wu and Rajaratnam 1996). Guan et al. (2014) showed that the approach flow is accelerated at the crest of the weir and a dead water zone forms immediately downstream of the dam. Moreover, secondary currents were detected that lead to rotating cells at the sides of the channel downstream of the dam. Ridges were detected in upward motion areas and erosion in downward motion areas (Guan et al. 2014; Meftah et al. 2004).

Additional governing parameters of the scour process to the one from the pier-like structures are water level difference between upstream and downstream of the structure Δh (= h_1 – h_2), tailwater depth h_2, overflow height over the structure $h_ü$ for flow parameters and height of the structure h_s, length of structure l_s for u-shaped dams for geometrical parameters (Meftah et al. 2004; Pagliara and Kurdistani 2013; Wang et al. 2019). The resulting scour pattern show a small scour hole upstream of the dam and a small dune downstream of the dam (Guan et al. 2014). The scour depth gradually increases until a maximum scour depth is reached at 2.5 w downstream of the dam.

2.4. Backwater rise

All of the beforementioned structures cause a scour hole and are possible measures to provide a suitable habitat. Nevertheless, the structures obstruct the flow and cause resistance which leads to a backwater rise which can increase the risk of inundations during flood events. Therefore, knowledge about the influence of the structures on backwater rise is needed.

The overall drag induced by in-stream structures is mostly caused by flow separation, vortices, turbulence, overfalling jets (for submerged structures) and hydraulic jumps. In free surface conditions, the energy loss results in a water surface elevation, with consequent backwater rise. The backwater rise Δh is defined as the difference between the upstream h_1 and downstream flow depth h_2 (Azinfar and Kells 2008, 2009). In literature the backwater rise of in-stream structures is addressed by different approaches:

I. In the energy approach the resistance is interpreted as a local loss h_v and incorporated through a local loss coefficient $h_v = \zeta \cdot \frac{U_2^2}{2g}$. Gebhardt et al. (2012) used this approach to describe the energy loss at a so-called Jambor weir sill where the loss coefficient was replaced by $\zeta = C_D \cdot \frac{w}{y_2}$ which leads to

$$\frac{\Delta h}{h_2} = \frac{Fr_2^2}{2} \cdot \left(1 - \left(\frac{h_2}{h_1}\right)^2 + C_D \cdot \frac{w}{h_2} \cdot \left(\frac{h_2}{h_1}\right)^2\right) \quad (1)$$

II. An empirical approach was used by Schalko et al. (2018) to investigate the backwater rise due to large wood accumulations. Based on previous studies and systematic experimental work the governing parameters were identified.

III. The momentum approach relates the resistance of the in-stream structure to a drag force that is employed on the flow. Through the use of a control volume the momentum approach avoids quantifying the individual energy losses and is therefore the most used approach for the description of backwater rise (Suribabu et al. 2011). Based on the momentum and continuity equation Azinfar and Kells (2008) derived an equation for backwater rise.

$$2\ Fr_1^2\left(\frac{h_1}{h_2}\right)^3 - \left(2\ Fr_1^2 - C_D A_r Fr_1^2 + 1\right)\left(\frac{h_1}{h_2}\right)^2 + 1 = 0 \quad (2)$$

C_D values have been derived e.g. for spur dikes (Azinfar and Kells 2008, 2009; Oak 1992) and for piers (Roberson and Crowe 1993).

The backwater rise of piers is dependent on the type of flow, discharge, geometrical boundaries of the cross section and pier shape (Charbeneau and Holley 2001; El-Alfy 2006; Suribabu et al. 2011; Yarnell 1934).

Yarnell (1934) derived an equation for the backwater rise of bridge piers. Suribabu et al. (2011) added a correction factor μ to Yarnell's equation to take more pier shapes and different blockage ratios A_r into account (e.g. square pier μ = 0.2 and 0.18 and CP μ = 0.24 and 0.2 for blockage ratios A_r of 0.33 and 0.4, respectively).

$$\frac{\Delta h}{h_0} = \mu\ K(K + 5Fr^2 - 0.6)\left(A_r + 15A_r^4\right)Fr^2 \quad (3)$$

K pier shape factor according to Yarnell: circular nose = 0.9, triangular nose = 1.05, square nose = 1.25.

El-Alfy (2006) investigated different pier shapes and found that the driving parameters for backwater rise are the blockage ratio and the Fr_2/Fr_{2c} ratio. The backwater rise can be calculated with the following equations:

$$\text{Rectangular pier}: \frac{\Delta h}{h_2} = 0.217 - 0.367\ C_r + 0.389\ Fr_2 \quad (4)$$

$$\text{Triangular pier}: \frac{\Delta h}{h_2} = 0.205 - 0.338\ C_r + 0.322\ Fr_2 \tag{5}$$

$$\text{Circular pier}: \frac{\Delta h}{h_2} = 0.178 - 0.315\ C_r + 0.314\ Fr_2 \tag{6}$$

C_r is the contraction ratio w_s/w and application range of Fr_2 = 0.2–0.62, C_r = 0.42–0.9 and pier length-width 5:1–30:1. It is to be noted, that the pier length-width ratio lays outside of the piers used in this study.

Azinfar and Kells (2008, 2009) investigated the backwater rise of spur dikes and identified the approach Froude number, the blockage ratio, the aspect ratio (height to length), the submergence and the angle of attack as the governing parameters. The increased drag coefficient was attributed to an increased negative pressure downstream of the structure for larger blockage ratios. Laboratory tests with fixed-bed conditions showed that the influence of the blockage ratio is one order of magnitude higher than the other components.

$$C_D = 1.62(1 - A_r)^{-2.40}\left(\frac{P}{L}\right)^{-0.32}\left(\frac{h_1}{P}\right)^{-0.19} \tag{7}$$

The maximum drag coefficient occurs for a submergence ratio between 1 and 1.5. The angle of 90° to approach flow direction showed the maximum drag coefficient while it is decreasing for smaller and higher angles. C_d increases significantly with the blockage ratio for unsubmerged conditions.

Gebhardt et al. (2012) studied the influence of backwater rise of Jambor weir sills and found the governing parameters to be the downstream Froude number, defined as $u_2/(g\ h_2)^{0.5}$, and the ratio h_2/w. They derived a design chart to identify the $\Delta h/h_2$ dependent on Fr_2.

Most investigations on backwater rise have been conducted under fixed bed conditions. Therefore, the effect of the scouring process around the in-stream structures on the backwater rise has not been considered in the studies presented up to this point. A scouring process leads to an enlargement of the flown through area and hence to lower flow velocities around the structure. Due to the altered flow field the drag of the structure changes and can lead to lower backwater rise under movable bed conditions. Schalko et al. (2019) conducted experiments under fixed and movable bed conditions to characterize the influence of the movable bed on backwater rise. The movable bed lead to a reduction of backwater rise $\Delta h/h_0$ of 25%.

3. Experimental methods

Two typical rivers in the South German Scarplands were used as a reference to the hydraulic and morphological boundary conditions of the experimental work. The landscape of Scarplands is characterized by escarpments. According to LAWA classification (Umweltbundesamt 2016) the river Murg, with its source in the Black Forest, is a silicate low mountain range river rich in fine to coarse sediment and the river Kocher, with its source in the Swabian Jura is a large river of the low mountain range, both part of the river catchment of the Rhine. The region is characterized by a disturbed hydrological regime (Leibundgut and Steinbrich 2002), a disturbed sediment balance and colmated river beds (Seitz 2020). According to the experience from previous projects, the morphological activity in those rivers starts at bankful discharge which is often reached at HQ2 (2-year return period).

The physical experiments were conducted with a model scale of roughly 1:25 to the prototypes, in a 8 m long and 0.79 m wide flume with a slope of 0.003, at the Theodor-Rehbock Laboratory of Karlsruhe Institute of Technology (KIT). The discharge of 31 l/s, which equals a discharge slightly lower than HQ2 and the waterlevel of 6.9 cm were selected according to the gauging station in the project reach. The uniform bed material ($\sigma_g = d_{60}/d_{10} = 1.3$) with a mean diameter of d_{50} = 3.1 mm was selected, so that clear-water scour conditions ($\tau_0/\tau_c < 1$) were ensured. The flume consists of three sections, an upstream fixed bed, a sediment pit including the measurement section and a downstream fixed bed (see Figure 3). The roughness of the fixed bed was similar to the movable section in the sediment pit.

To ensure the same starting and ending conditions for each experiment, a detailed experimental procedure was developed. Sediment was introduced dry into the flume and with the help of a sprinkling machine watered until saturation. A protection plate covered the saturated sediment and the water level rose until the target value. Further on, the inflow rate was slowly raised while the tailgate was lifted simultaneously to maintain the water level. The protection plates were removed carefully when the desired discharge and water level was reached. Once equilibrium was reached, the pump was slowly shut down and the tailgate gradually closed to maintain the water level. Through a drainage system in the bottom of the flume, the water was thus drained out of the flume over several hours to prevent any more sediment motion and preserve the existing bed morphology.

During and after the experiment, discharge, water level, flow velocities at selected points and bed

morphology were measured. The inflow rate was measured with an electromagnetic flow meter with an accuracy of ±0.1 l/s. The water level was measured with ultrasonic sensors with an accuracy of ±0.2 mm and were located 5 h_0 and 8.8 h_0 upstream and 5 h_0 downstream of the structure. The flow velocities were measured with Laser-Doppler-Anemometry. The bed morphology was documented using a Structure from Motion technique. With this photogrammetric technique, a three-dimensional topography can be derived through two-dimensional images (Morgan et al. 2017). Between 250 and 300 photographs were taken in a prescribed procedure and calibrated with 10 calibration points in the flume. *Agisoft Metashape* was used to transform the images into a 3D point cloud (Agisoft Metashape 2020). 2.1 billion points could be detected in the measurement section of 2.1 m × 0.79 m with an accuracy of ±1 mm. Three replicates of the bed morphology were captured for each structure to be able to quantify the sensitivity of the experimental setup. The results which are shown in terms of bed morphology refer to the average of these three replicates.

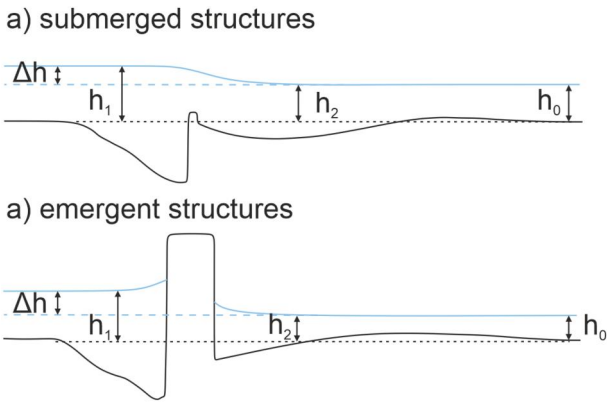

Figure 2. Definition of parameters in the context of backwater rise: upstream water level h_1, downstream water level h_2, backwater rise Δh and associated water depth for uniform flow conditions h_0.

As mentioned above, three groups of structures were tested in the flume (see Figure 1). The pier-like structures consisted of a circular pier (CP), a rectangular pier (RP) and a triangular pier (TP). These structures are emergent and have a width of 15.8 cm which equals 20% of the total flume width w. The tested stone-like structures were the Double Wing Deflector (DWD) and the Deflected Groyne (DG). The DWD consists of two triangular submerged groynes with a width of each 0.4 w and an initial offset of 0.1 w. The DG covers 1/3 w. The Kdam covers the whole width of the flume and has a notch in the middle of the flume. The last three structures are submerged and the height of the structure h_s is 0.41 h_0 above the initial bed which equals a water level that is reached at MQ (mean discharge).

3.1. Time development and equilibrium conditions in bed morphology processes

For the comparison of the bed morphology of different structures, it is essential to ensure the same boundary conditions. The basis for comparison is the so-called equilibrium state which was defined according to the criterion presented by Kannen et al. (2022). This equilibrium criterion is based on

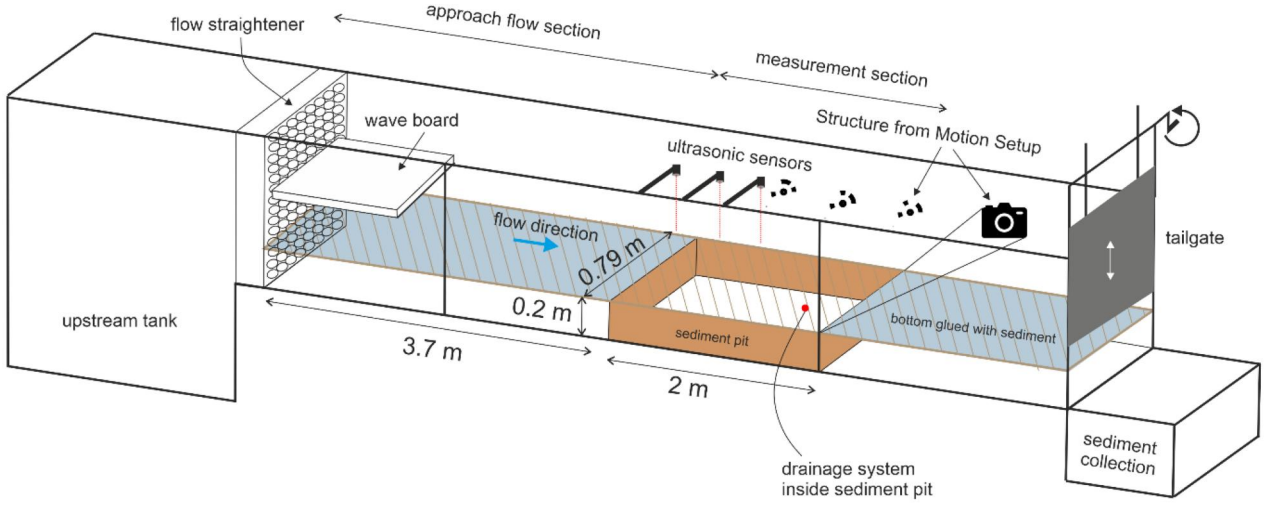

Figure 3. Experimental setup of the clear-water scour experiments: discharge comes from an upstream tank and flows through a flow straightener and the surface waves are tranquilized through a floating plate. After 3.7 m, a sediment pit with movable bed is installed which represents the measurement section. The measurement section is equipped with three ultrasonic sensors for continuous water level measurement. On the opposite side from the visualization window, markers and a camera are shown as part of the Structure from Motion setup. The fixed bed is glued with sediment in the same size as in the sediment pit to ensure equal roughness conditions. At the downstream end of the flume a liftable tailgate is installed to control the flow at the beginning of the experiments. Downstream of the flume the sediment is collected in a tank.

the scouring rate at the deepest point of the bed morphology; as soon as the scouring rate drops below 0.05 D within a time span of 24 h equilibrium is reached. D is the hydraulically significant length scale that is defined as $w_s{*}h_s/h_0$, to take emergent and submerged structures into account (cf. Kannen et al. (2022) for further details).

Figure 4 shows the time development at the deepest point at all structures, where time is normalized by the time to equilibrium obtained as above explained. Pier- and stone-like structures showed a linear and asymptotic behaviour whereof the stone-like structures (DWD and DG) showed a slower development in the first phase of the scouring process ($t/t_e = 0.25 - 0.5$). The dam-like structure shows a non-linear and non-asymptotic behaviour as explained above, which is attributed to the rather high limiting scour rate for the Kdam, and to the location of the deepest point at the flume walls instead in the centreline of the flume. Moreover, the physical phenomena that lead to scouring at a dam-like structure are fundamentally different from the other two types of structures, pier- and stone-like structures. The latter show big stable vortex systems, whereas the dam-like structure is considered as a constriction scour where scouring is induced partially through vortex systems but also due to increased bed shear stresses.

For comparison and verification, the time to equilibrium t_e and the corresponding equilibrium scour depth was calculated based on the criterion by Kannen et al. (2022) for various experimental studies with available measurement data (B. W. Melville and Chiew (1999) for CP, Rashak and Khassaf (2020) for DG, Guan et al. (2019) for Kdam and Coleman et al. (2003) for AB). The normalized time development of the scour depth is displayed in Figure 4. The values of the pier- and stone-like structures (CP, DG and AB) all lay within the same boundaries of the linear and asymptotic behaviour as the data measured within this study (see Figure 5). The values of dam-like structures from Guan et al. (2019) show a comparable deviation of this behaviour that is non-linear and non-asymptotic. As explained above, there are

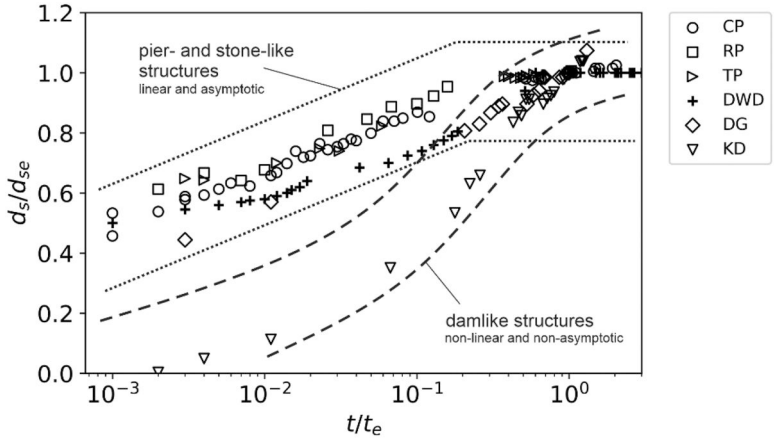

Figure 4. Temporal development of relative scour depth d_s/d_{se} for different flow types; time is normalized by the time to equilibrium t_e.

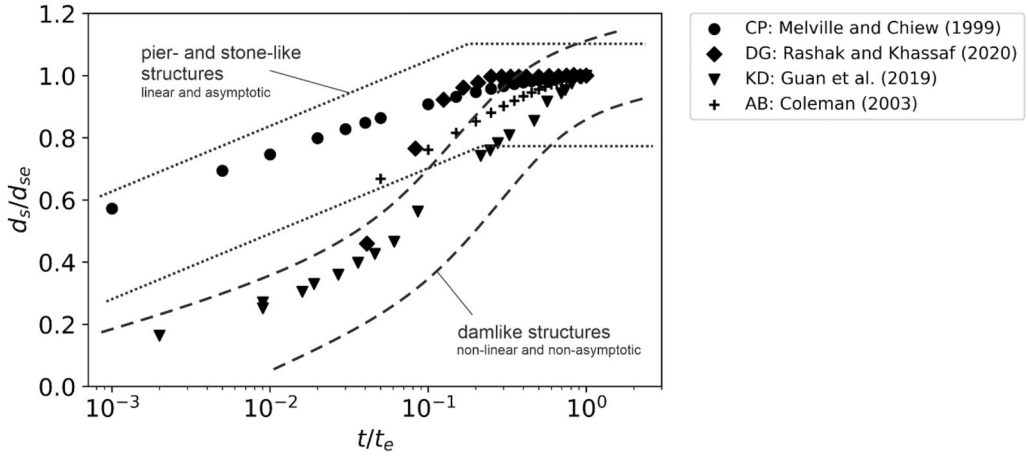

Figure 5. Application of the equilibrium criterion by Kannen et al. (2022) on time development data of various literature values of pier- ((B. Melville 2008) for CP and (Coleman et al. 2003) for abutments), stone- (Rashak and Khassaf 2020) and dam-like structures (Guan et al. 2019) presented in a semilogarithmic normalized diagram.

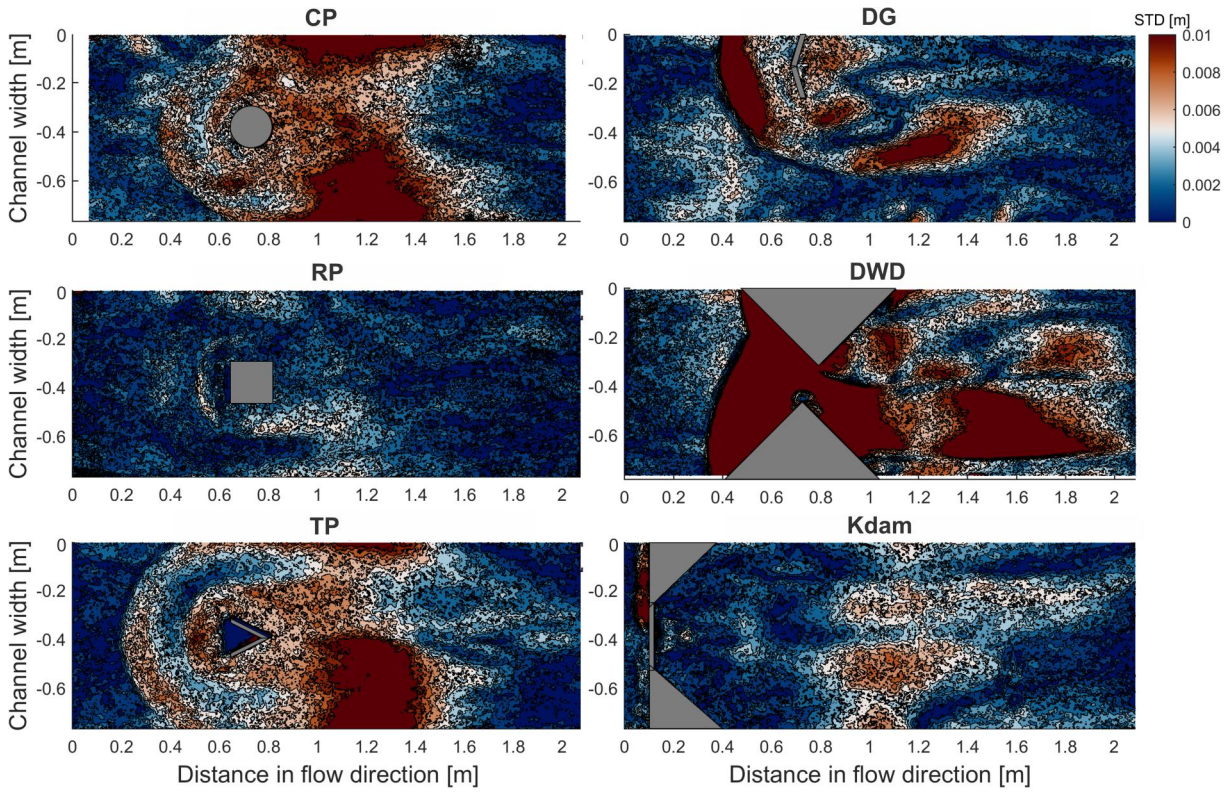

Figure 6. Standard deviation of bed morphologies for different structures in equilibrium stage (three replicates).

fundamental differences in the physical processes that lead to scouring around dam-like structures in contrast to pier- and stone-like structures. The scouring mechanism around pier- and stone-like structures is dominated by stable vortex systems like the horseshoe vortex system as explained in Section 4.4 whereas at dam-like structures a combined effect of vortex system and increased bed shear stresses due to a constriction is present.

4. Results

4.1. Reproducibility of the morphological experiments

The comparison of three experimental runs, above referred, provides information on the sensitivity and reproducibility in terms of scouring morphology and position of its main features. Figure 6 shows the standard deviation of a bed morphology in equilibrium stage. Since $d_{50} = 3.1$ mm all deviations ≤ 3 mm are interpreted as no changes.

Looking at the pier-like structures, it is noticeable that the RP shows the most reproducible equilibrium bed morphology. The highest standard deviation can be found downstream of the structures CP and TP. The scour hole dimensions are similar for all experimental runs for pier-like structures, indicated by a clear line where no more changes in bed morphology can be detected. Only in the slopes of the scour hole small differences in bed morphology are present. For stone-like structures, there is a diverse picture of the deviation from the average bed. DG has higher deviations in sections with higher slopes namely at the upstream and lateral end of the scour hole. The DWD shows the highest sensitivity regarding bed morphology. The Kdam shows good reproducibility which is a sign of a stable vortex system. Overall, all structures show the tendency of higher standard deviations downstream of the structure and in regions with high slopes, which are associated with sliding mechanisms. Nevertheless, the results are considered enough reproducible for our investigation and the bed morphology at equilibrium, which will be shown further, is the average of the three replicates.

4.2. Bed morphology and backwater rise at equilibrium stage

The average of the bed morphologies in equilibrium stage is displayed in Figure 7. The deepest scour position is located immediately upstream of all pier-like structures. The scour hole evolves circularly in upstream and lateral direction and shows a pronounced change in slope inside of the scour hole that is most prominent in TP case. The bed morphology is symmetrical with the centreline of the flume. Downstream of the pier, two deep lateral sections and a central dune can be identified in all pier-like cases. All pier-like cases show a wall-interaction, meaning that the scour hole reaches the flume walls and cannot evolve fully to the sides.

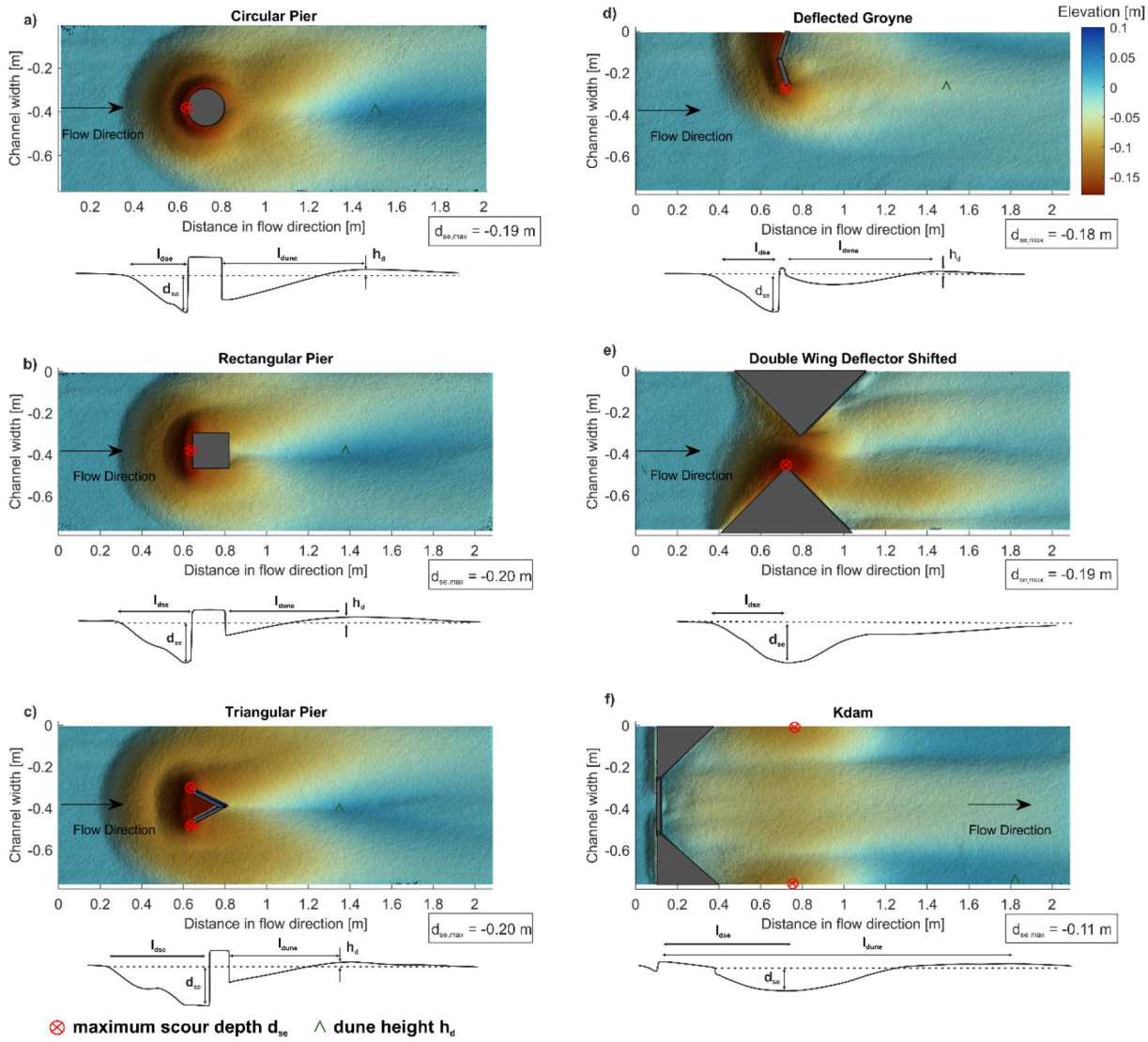

Figure 7. In the background: average of the bed morphologies at equilibrium stage for six different structures (three replicates). The maximum scour depth of each structure is indicated in red and the value is given in the attached box. Below every image the geometrical parameters of the scour holes are indicated: length of scour hole l_{dse}, distance of the dune l_{dune}, maximum end scour depth d_{se} and height of the dune h_d.

Since the engineering structures are supposed to be implemented in urbanized areas where riverbank protection is a common measure, there would be a riverbank interaction in natural conditions as well. Especially the reference rivers, where the measures are to be installed and in which this investigation is based, riverbank protection and levees prevent scouring at the sides. If interaction with the riverbank is not wanted, the width of the piers could be reduced. This would lead to smaller scour width, but also to smaller scour depth. The optimization of scour width to scour depth is up to further research.

The stone-like structures (DG and DWD) have the deepest scour position at the head of the structure. Visually we observed that the scour hole first develops towards upstream and lateral and later also downstream of the structure. Both structures show no symmetry since the geometries are also not symmetrical regarding the centreline of the flume. The DG is a one-sided structure, so the alterations in bed morphology concentrate on one side. At approximately $2\,l_s$ downstream of the DG there is an accumulation of sediment material and a dune is formed. The DWD is a two-sided structure and shows the deepest area around the upstream wing. Downstream of the DWD two deep sections can be identified.

The Kdam shows the smallest scour depth but a long deepening of the bed which reaches the end of the measurement section. At approximately 2/3 of the width of the structure w_s the deepest scour position is located at the flume walls.

Table 1. Geometrical parameter of the scour hole for the six tested structures.

	CP	RP	TP	DWD	DG	Kdam
t_e [h]	48	24	48	48	72	96
d_{se} [cm]	19.2	20.1	19.9	19.1	18.3	10.9
l_{ds} [cm]	30.2	35.3	44.3	36.6	35.4	(114.1)
l_{dune} [cm]	75.7	62.6	59	–	75	168.5
h_d [cm]	2.93	2.75	2.3	–	1.3	1.8

Table 2. Normalized backwater rise provoked by different hydraulic structures in a movable bed at equilibrium conditions.

Structure	$\Delta h/h_2$ [%]	$\Delta h_1/h_0$ [%]
CP	4.7	7.4
RP	4.2	15.7
TP	7.2	10.5
DWD	0.9	13.4
DG	–	6.9
Kdam	27.1	31.8

Table 1 and Figure 7 summarize the geometrical parameters of the scour hole for all structures. Except for the Kdam, d_{se} lays within a range of 2 cm (~10% of total depth). The Kdam differs with only half of the scour depth. For pier-like structures the scour hole increases for CP to RP to TP. With increasing length of the scour hole the distance of the dune is decreasing. With increasing distance of the dune, the height of the dune increases. For stone-like structures the length of the scour hole is comparable to the RP. The distance of the dune for DG is 1.34 w_s and the dune height is smaller than for the piers. For the Kdam l_{ds} and l_{dune} lay both downstream of the structure. The length of the scour hole and also the distance of the dune are significantly higher than for all the other structures.

To assess the flood risk, the backwater rise, $\Delta h/h_2$, in equilibrium stage is analysed (cf. Figure 2 for the definition of Δh). The pier-like structures all showed a normalized backwater rise $\Delta h/h_2$ between 4% and 8%. The DWD showed a very small normalized backwater rise of 0.9%. For the DG a water level drop could be detected which is not a physically feasible result. The authors attribute this to a standing wave that was interfering with the mean water level and is therefore not considered in the further analysis. The dam-like structure (Kdam) showed a substantial normalized backwater rise of 27.1%. The changes in comparison with the uniform water level h_0, were evaluated through the relation $\Delta h_1/h_0 = (h_1\text{-}h_0)/h_0$. $\Delta h_1/h_0$ lays within 7 and 16% for pier- and stone-like structures and is high for dam-like structures with 31.8% (see Table 2).

4.3. Visual observations of the flow field in equilibrium stage

The beforementioned bed morphologies can be explained by the flow field that develops around the different structures (see an interpretation in Figure 8). The flow field around a pier is well-known. Upstream of the pier a surface roller and a downflow that reaches the bed start the scouring process. A horseshoe vortex evolves around the pier that is the main driver for sediment transport out of the scour hole. Downstream of the pier wake vortices advance until far downstream. As the scour hole evolves sediment slides down the upstream slope and is transported downstream by the horseshoe vortex. In the deep lateral sections, sediment transport happens through rolling and hopping mechanisms. The wake vortices downstream of the pier rotate in opposite directions and accumulate part of the sediment in a downstream dune. In equilibrium stage, there is little sediment motion.

At the stone-like structures scouring initiates at the head of the structures (groyne head). The main drivers for sediment erosion are a helix upstream of the groyne and a stable rotating eddy which is located immediately downstream in the lee of the structure. The upstream hole evolves by sliding of the sediment. In the deep sections downstream of the structure, the sediment motion can be characterized as rolling and hopping. As the equilibrium stage approaches, the strength of the eddy reduces and the sediment entrainment weakens.

The Kdam shows four rotating vortex systems in the flume. Within these rotating vortices the sediment moves by rolling and hopping mechanisms.

4.4. Evaluation of water depth and distribution of scours as deep pool habitat according to LSGÖ

Within the LSGÖ (A. Becker and Ortlepp 2022), a deep pool habitat is characterized by a water depth of greater than 2 m on an area of at least 6 m^2, and a flow velocity preferably between 0.3 and 0.6 m/s. When considering a reference river at the model scale in which this investigation is based, a length of 2 m corresponds to 8 cm, and an area of 6 m^2 corresponds to 96 cm^2. Figure 9 shows the distribution of the area of the scour in the target depth of at least 8 cm. The target depth could be reached for all structures. For the pier-like structures the area is in front and lateral to the structure. In case of the CP and TP the area extends downstream into two deep lateral sections. The extension of the deep sections is longest for TP. The suitable areas around the stone-like structures extend from the head of the structure. The DWD shows an elongated suitable zone on the right side. The suitable areas for the Kdam are on both riverbanks.

5. Discussion

5.1. Bed morphology at equilibrium stage

Figure 10 shows the bed morphology of CP and RP in comparison with literature values from Dey and Raikar (2007). The bed morphologies were normalized with the hydraulically significant length D as defined in Kannen et al. (2022). The hydraulically significant length D (= w_s * h_s/h_0) is a length scale

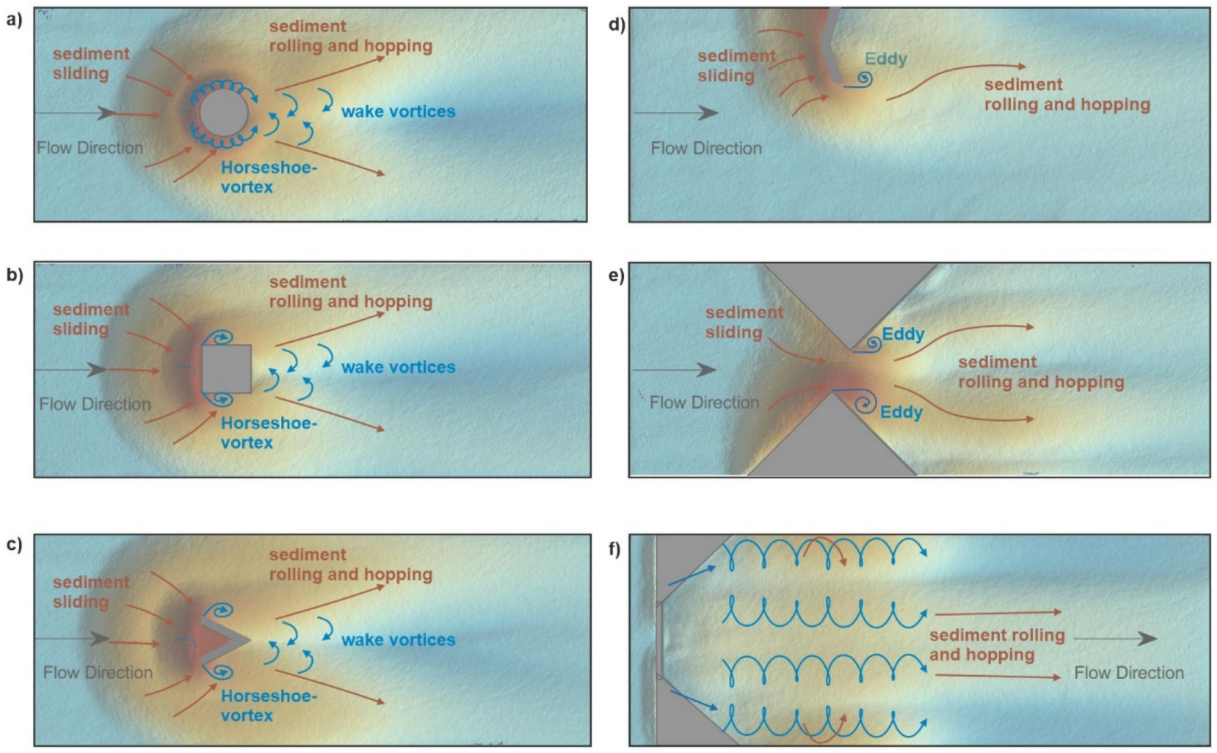

Figure 8. Interpretation of visual observations of the flow field (blue) and sediment motion (brown), for the different structures during the scouring process. The background represents the bed morphology at equilibrium stage and is shown for visual orientation.

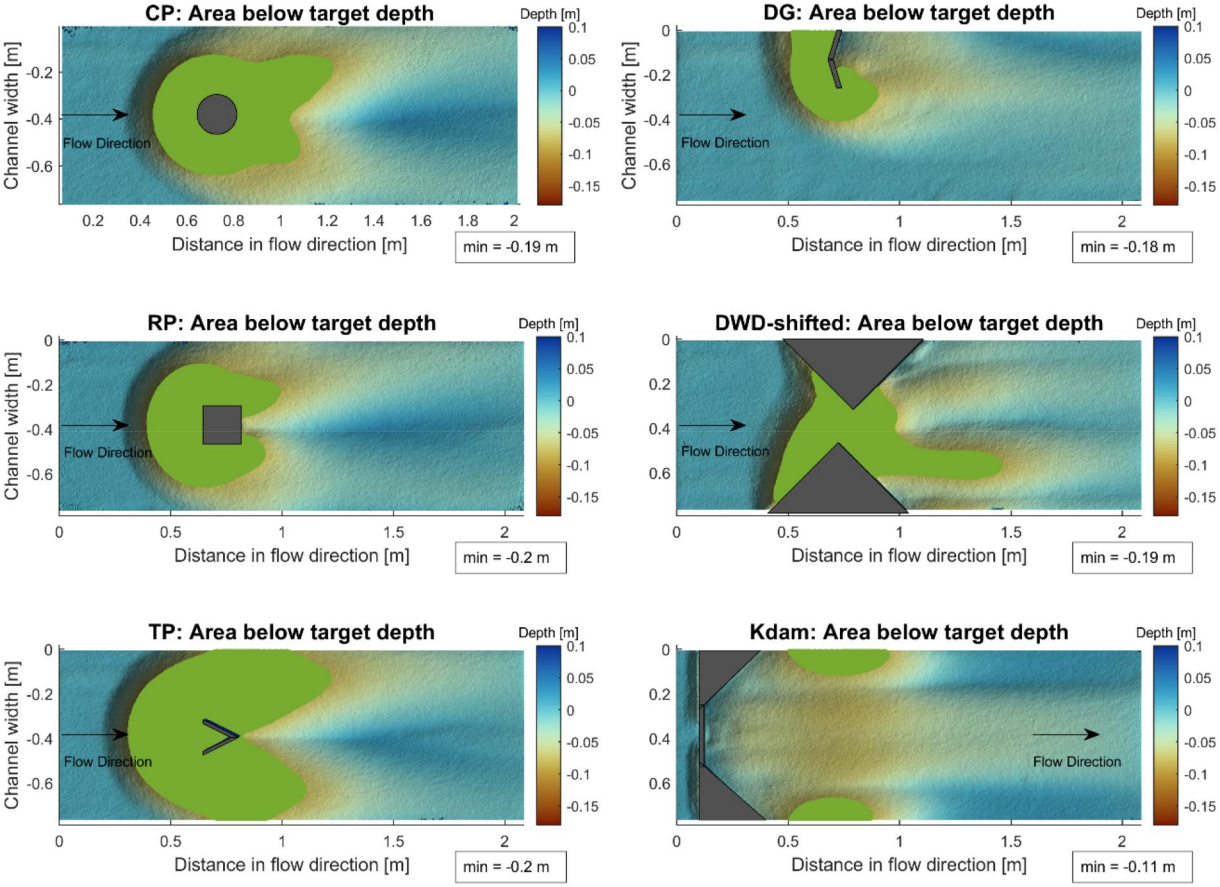

Figure 9. Distribution of the area of the scour in the target depth of 8 cm, which is considered a suitable depth for a deep pool habitat, according to the application of LSGÖ guidelines and when reduced to the physical model scale. This means the indicated areas (in green) are possible suitable habitats if the flow field is suitable accordingly.

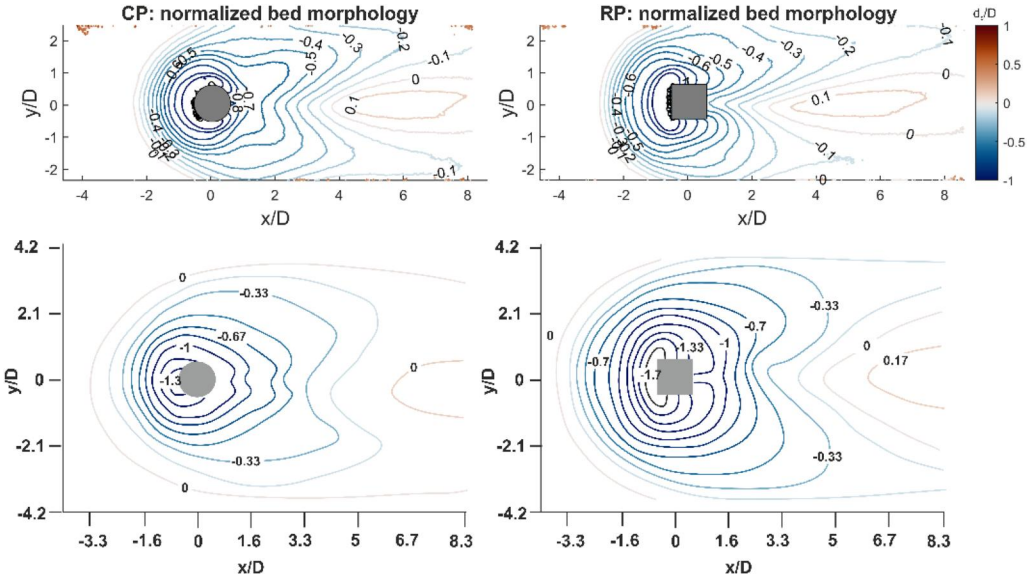

Figure 10. Comparison of normalized bed morphologies of this study (above) with values from (Dey and Raikar 2007) for CP (left) and RP (right).

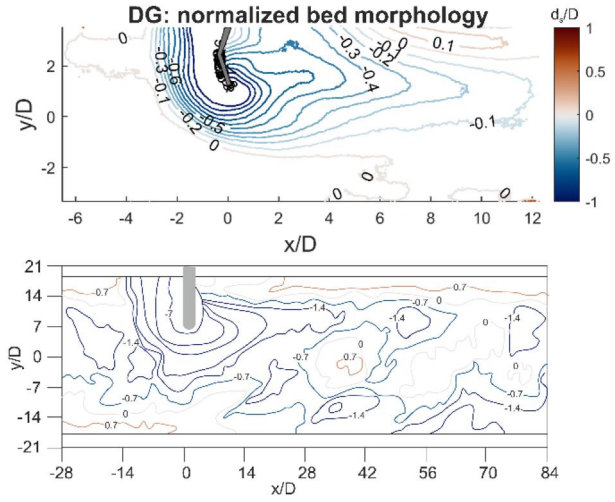

Figure 11. Comparison of normalized bed morphologies of this study (above) with values from Harada et al. (2013) for DG.

that is significant for the scour process, for pier-like structures e.g. the pier width ($h_s = h_0$, therefore $D = w_s$) and for stone-like structures a relative water depth is added to account for the submergence of the structure.

The data from this study and from Dey and Raikar (2007) show similar scour patterns, the deepest scour position is located upstream of the pier and two deep lateral sections evolve further downstream. A central dune forms downstream of the pier. Both, the data from this study and from Dey and Raikar (2007) demonstrate that RP produces a deeper scour hole. Moreover, a shift of the beginning of the dune towards the pier from $x/D = 3.8$ for CP to $x/D = 2.2$ for RP can be detected in this study as well as in the data of Dey and Raikar (2007) with a shift from $x/D = 6.7$ at the CP to $x/D = 4.8$ at RP. The differences in relative scour depth d_s/D can be attributed to the difference in the relative sediment size D/d_{50} and to the flow shallowness h_0/D. Dey and Raikar (2007) have a relative sediment size of $D/d_{50} = 148$ and in this study, it is 50. According to Melville (2008) the relation of relative scour depth d_s/D to relative sediment size D/d_{50} shows a peak at D/d_{50} of 50 and has decreasing trends for values over and under 50. The sediment in Dey and Raikar (2007) can be classified as fine sediment whereas the present experimental setup is located at the tipping point of fine to coarse sediment. The flow shallowness h_0/D can also influence scour depth. The setup of Dey and Raikar (2007) is classified as a narrow pier ($h_0/D = 2$) and therefore scour depth is independent of water depth (B. Melville 2008). In the case of this study, the flow shallowness h_0/D is 0.42 which lays in the section of intermediate length where relative scour depth d_s/D is dependent on pier width D and on water depth h_0.

A comparison of the DG in this study to literature data of Harada et al. (2013) shows that the deepest point of both is located at the head of the groyne (Figure 11). The scour hole expands laterally in upstream direction up to x/D = 3 in the present case and x/D = 14 in Harada et al. (2013). In downstream direction, the scour hole extends up to x/D = 12 in the present case and x/D = 70 in Harada et al. (2013). The dune starts at x/D = 5.5 in the present case and immediately downstream of the groyne in Harada et al. (2013). The differences in relative scour depth can be attributed to (I) the different sediment size D/d_{50} = 1.18 in Harada et al. (2013) and D/d_{50} = 35.8 in this study which classifies both setups as coarse sediment and (II) to relative submergence h_s/h_0 with 0.41 in the present case and 0.07 in Harada et al. (2013).

The Kdam is compared to a submerged weir as shown in Guan et al. (2014) in Figure 12. Both bed morphologies show a slight erosion upstream of the dam. Immediately downstream of the dam a slight dune can be observed in Guan et al. (2014) that is not detectable in this study which is probably due to the different downstream geometries of the structures. The deepest scour position is located at the flume walls for both cases. The relative scour depth is d_s/D = 1.3 in Guan et al. (2014) and 0.3 in the present case. The difference in flow intensity (U_0/U_c = 0.87 in Guan et al. (2014) and 0.9 in the present case), the overtopping ratio (h_s/h_0 = 0.33 for Guan et al. (2014) and 0.4 for this study) and the relative sediment size (D/d_{50} = 105 for the present case and D/d_{50} = 137 for Guan et al. (2014) which leads to the classification "fine sediment") would indicate a higher relative scour depth for the present case and therefore would indicate the opposite trend as the one which is observed. The differences in relative scour depth are therefore attributed to the different observed flow fields. Guan et al. (2014) observe a recirculation zone downstream of the submerged weir and two transversal circulating cells (w/h_0 = .9). In this study, four circulating cells have been observed (w/h_0 = 11.6). It is expected that the strength of two big cells is higher than four small ones and therefore the relative scour depth is higher in Guan et al. (2014). This hypothesis is supported by the fact that the transversal cross profile in Guan et al. (2014) shows one peak in the centre and the cross profile in this study shows 2 peaks at 1/4 and 3/4 of the flume width.

The Kdam is commonly utilized for bed stabilization in degraded river systems; however, it has shown limited effectiveness for the specific objective under investigation. It is crucial to define the purpose of an in-stream structure before its installation, as different structures yield varying outcomes. While Kdams are not inherently unsuitable as in-stream measures, they do not effectively achieve the goal of creating deep pool habitats. This conclusion highlights the importance of aligning in-stream structures with their intended uses to ensure desired ecological outcomes.

5.2. Backwater rise at equilibrium stage

Especially in urbanized areas, it is important to quantify the backwater rise during flood caused by the implementation of in-stream structures. Figure 13 shows the mean value of three experiments for the backwater rise, as a function of the downstream Froude number, for different structure types. The stone-like structures show the lowest, the pier-like

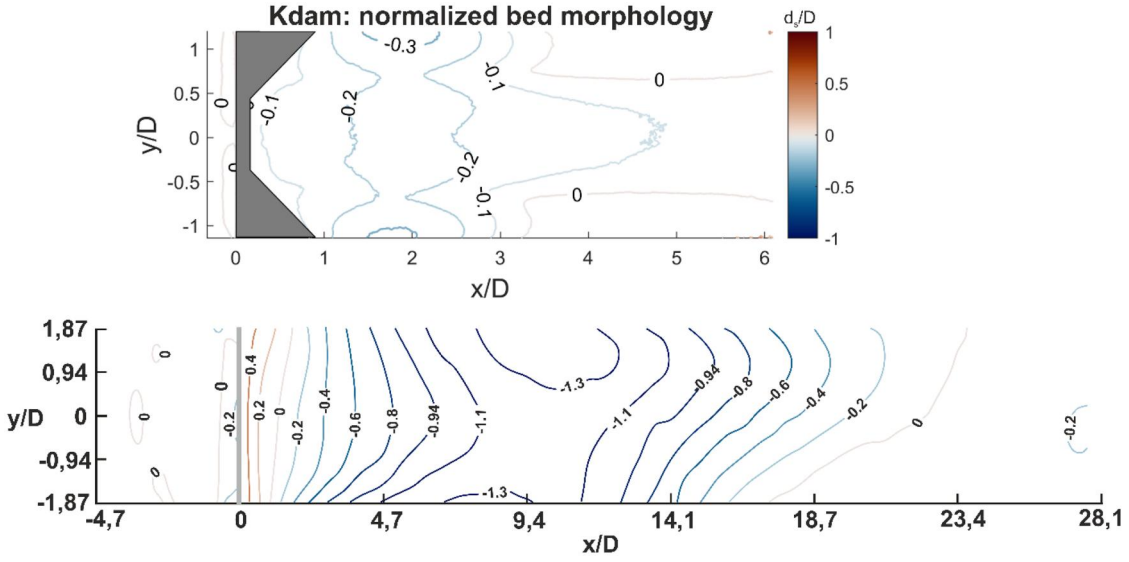

Figure 12. Comparison of normalized bed morphologies of this study (above) with literature values from Guan et al. (2014) for Kdam.

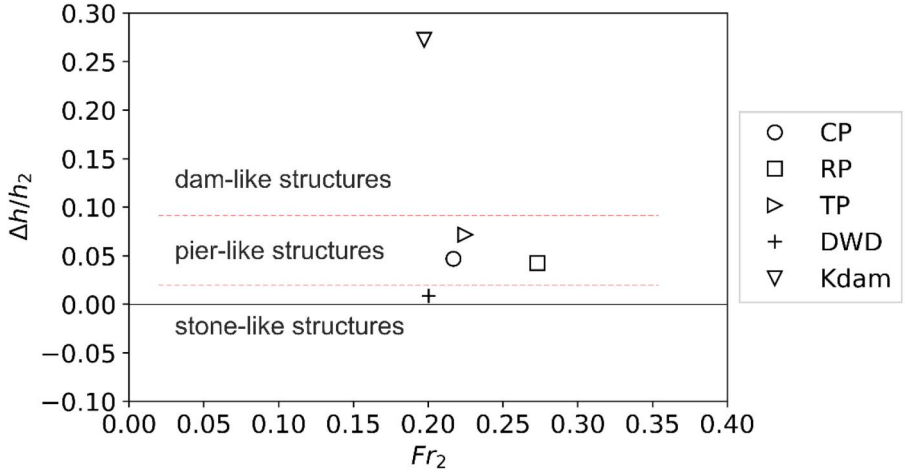

Figure 13. Mean values of backwater rise $\Delta h/h_2$ for different flow types (three replicates).

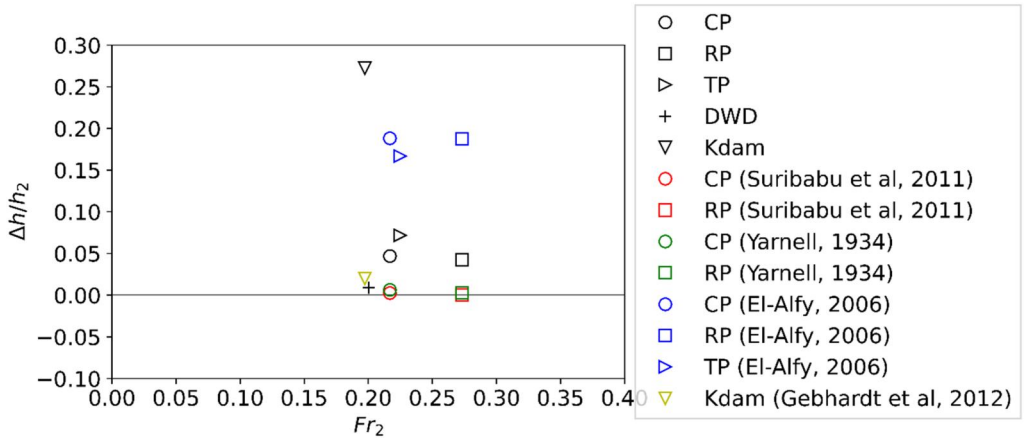

Figure 14. Comparison of the backwater rise of different flow types with literature values.

structures an intermediate and the dam-like structure shows the largest backwater rise. The difference in backwater rise can be attributed to the different flow types. Consequently, this means, that solely overflown structures induce higher backwater rise than those which are flown around both sides and divide the flow. Structures which are overflown and do not occupy the whole river width produce the smallest backwater rise.

Literature values for pier-like structures as shown in El-Alfy (2006), Suribabu et al. (2011) and Yarnell (1934) demonstrate that the backwater rise $\Delta h/h_2$ has not been characterized consistently yet and differs in one order of magnitude (see Figure 14). The equations of Suribabu et al. (2011) and Yarnell (1934) predict significantly lower backwater rise than the equation of El-Alfy (2006). The values measured in this study lay in between the two literature sources. The values for the dam-like structures differ significantly from literature values of Gebhardt et al. (2012) which is probably due to the optimized Jambor weir sill geometry that reduces backwater rise significantly.

The literature study showed that the blockage ratio is the most influencing parameter on backwater rise (Addy and Wilkinson 2016; Suribabu et al. 2011). Until now most studies were performed under fixed bed conditions where the blockage ratio A_r is defined as:

$$A_r = \frac{A_s}{h_1 w} \tag{8}$$

For movable bed conditions. the bed morphology changes and hence the flown through area and consequently also the blockage ratio changes over time. Figure 15. shows the definition of the different areas during the scouring process. In the initial stage, A_{so} is the frontal projection of the solid area and A_{fo} the flown through area without considering the structure. During the scouring process the bed is eroded and the flown through area increases until equilibrium time t_e is reached. A_{fe} is the flown through area in equilibrium stage. At the same time, the structure gets more exposed to the flow with an area A_{se}. For further analysis the blockage ratio during equilibrium conditions is defined as (Figure 15):

$$A_{re} = \frac{A_{se}}{A_{fe}} \tag{9}$$

The drag coefficient C_D is calculated with equation (7) (Azinfar and Kells 2009) with the beforementioned blockage ratio A_{re} and is shown in Figure 16.

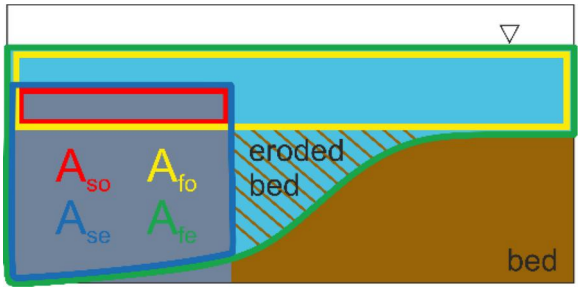

Figure 15. Definition of solid and flown through areas in initial stage (A_{so} and A_{fo}) and in equilibrium stage (A_{se} and A_{fe}).

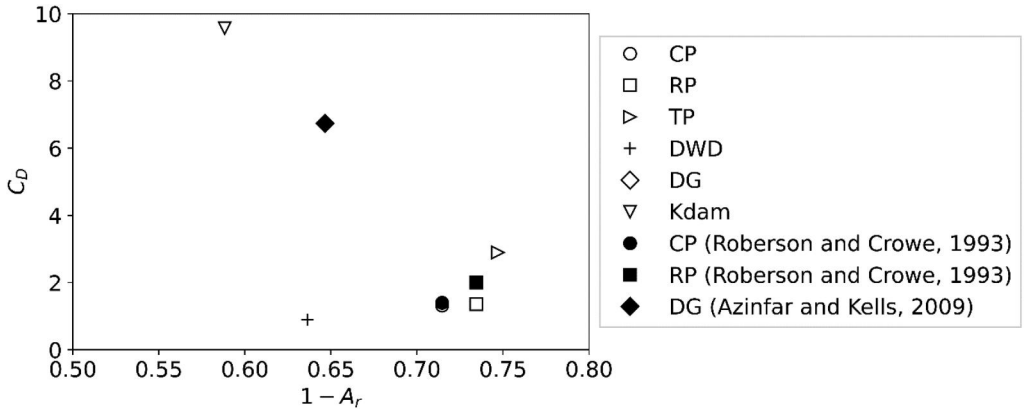

Figure 16. Comparison of the drag coefficient C_D of different flow types with literature values.

The stone-like structures show the lowest C_D values, the pier-like structures intermediate and the dam-like structures show the highest drag coefficient at equilibrium. The pier-like structures CP and RP are in good comparison with literature values from Roberson and Crowe (1993).The differences in the measured backwater rise and the literature values can have several reasons. A reason could be that most studies were performed under fixed bed conditions, so that the mechanisms explained in chapters 4.2 and 4.3 cannot take place, thus much lower C_D values can be expected. Schalko et al. (2018) estimated a difference in backwater rise of 25% between fixed and movable bed conditions.

5.3. Evaluation of scours as deep pool habitat according to LSGÖ

The calculation of geometrical parameters of the scour holes reveals that the area at target depth of 8 cm A_{target} which is indicated in Figure 17(a) is greatest for the TP and smallest for the Kdam. The ratio A_{target}/A_0 provides a measure of the benefits obtained by the scour hole (see Table 3). The ratio lays between 0.06 and 0.39 and is small for dam-like structures and high for pier-like structures. To characterize the scour holes of the different structures the distribution of area and volume over the scour depth were analysed. With increasing depth, the area of the scour hole decreases asymptotically. For stone-like structures the decrease is most pronounced with an area reduction of approx. 0.8 in a scour depth of 0.3 of the total scour depth. For dam-like structures, the reduction is 0.40. It can be concluded that stone-like structures create small but deep and dam-like structures big and flat scour holes. The geometry of pier-like scour hole lays in between (see Figure 17a).

The beforementioned numbers refer to clear-water scour conditions at an approximate HQ2 and bed shear stresses right below threshold conditions. Discussion may arise whether lower discharges lead to a redeposition of sediment inside the scour hole. Lower discharges also lead to lower bed shear stresses and only smaller sediment fractions are in motion. The flow field inside the scour hole is persistent also for lower discharges and approach flow velocities, hence no considerable amounts of redeposition are expected. At latest with the next HQ2 the sediments will be removed from the scour hole. Moreover, changes in morphology are naturally varying due to varying discharges and can be expected over the whole river reach.

To estimate how many fish can be hosted inside a scour hole, the distribution of cumulated volume over depth is displayed in Figure 18. With increasing depth, the cumulated volume increases. The total volume V_{tot} of the scour is highest for TP and lowest for the DG. The target volume V_{target} is the cumulative volume below the target depth. The ratio V_{target}/V_{tot} indicates how much volume is below target depth and hence can be classified as a suitable

habitat. The range is between 0.11 and 0.19 (except Kdam with 0.02, see Table 3).

Even though the intention was to create deep pool habitats the results show that the implementation of in-stream structures can create additional possible habitat types. The possible suitable areas were identified by an interpretation of the bed morphology and flow field results. On the example of the TP the further benefits are explained (see Figure 19). The area identified by 0 in Figure 19, immediately upstream of the TP, is not suitable as it has a significant downward flow component which is not associated suitable by most fish species (Muhawenimana et al. 2019; Tritico and Cotel 2010). The areas 1 at the lateral ends of the TP have mainly velocity components in main flow direction and therefore are suitable as deep pool habitat. The dune that forms in the centre (area 3) could possibly be, in the presence of a suitable bed sediment, a gravel bar that could serve as spawning habitat (A. Becker and Ortlepp 2022). Since there is a gradient from the dune towards the deep pool there are areas with medium flow velocity and a gentle slope (area 2) (A. Becker and Ortlepp 2022). In total, the surrounding of the TP could be a very vital living environment from a spawning habitat in the gravel bar (3) for larvae fish, a gently sloped area (2) for juvenile fish and a deep pool for adult fish. The deep pool habitat also represents a resting zone after the spawning process of barbels. Due to the spatial proximity of the different habitat types, the TP can serve as a multifunctional habitat structure. The spatial interconnectedness of different habitat structures is crucial for fish species in order to complete their life cycle in rivers from larvae to adult fish (Kalogianni et al. 2020). Often missing or insufficient scour structures in rivers have the additional benefit of initiating further habitat functions.

Table 3. Area at elevation zero A_0, relative area in target depth A_{target}/A_0, area at the target depth of 8 cm in model and in natural scale $A_{target\ model/nature}$, volume below target depth in model and in natural scale $V_{target\ model/nature}$, and total volume of the scour below an elevation of zero V_{tot} and relative volume in target depth V_{target}/V_0 for different structures.

	CP	RP	TP	DWD	DG	Kdam
A_{target_model} [m^2]	0.26	0.20	0.47	0.21	0.10	0.07
A_0 [m^2]	1.03	1.07	1.19	1.10	1.02	1.17
A_{target}/A_0 [-]	0.25	0.19	0.40	0.19	0.0944	0.0574
$A_{target\ nature}$ [m^2]	164	127	295	130	60	42
$V_{target\ model}$ [m^3]	0.0103	0.0087	0.0158	0.0087	0.0042	0.0012
V_{tot} [m^3]	0.0631	0.0563	0.0818	0.0588	0.0386	0.06
V_{target}/V_{tot} [-]	0.16	0.15	0.19	0.15	0.11	0.02
$V_{target\ nature}$ [m^3]	160	136	247	136	67	19

6. Outlook

In Figure 19, we show how the placement of the derived in-stream structures can include an additional positive impact for the deep pool habitat. The in-stream structure is positioned at the confluence of a tributary of a small cold water mountain stream into a bigger river of the low mountain range with higher water temperature. During extreme low water and heat events the water temperature difference of the two rivers can have an additional positive influence on the deep pool habitat as it can provide lower water temperature inside

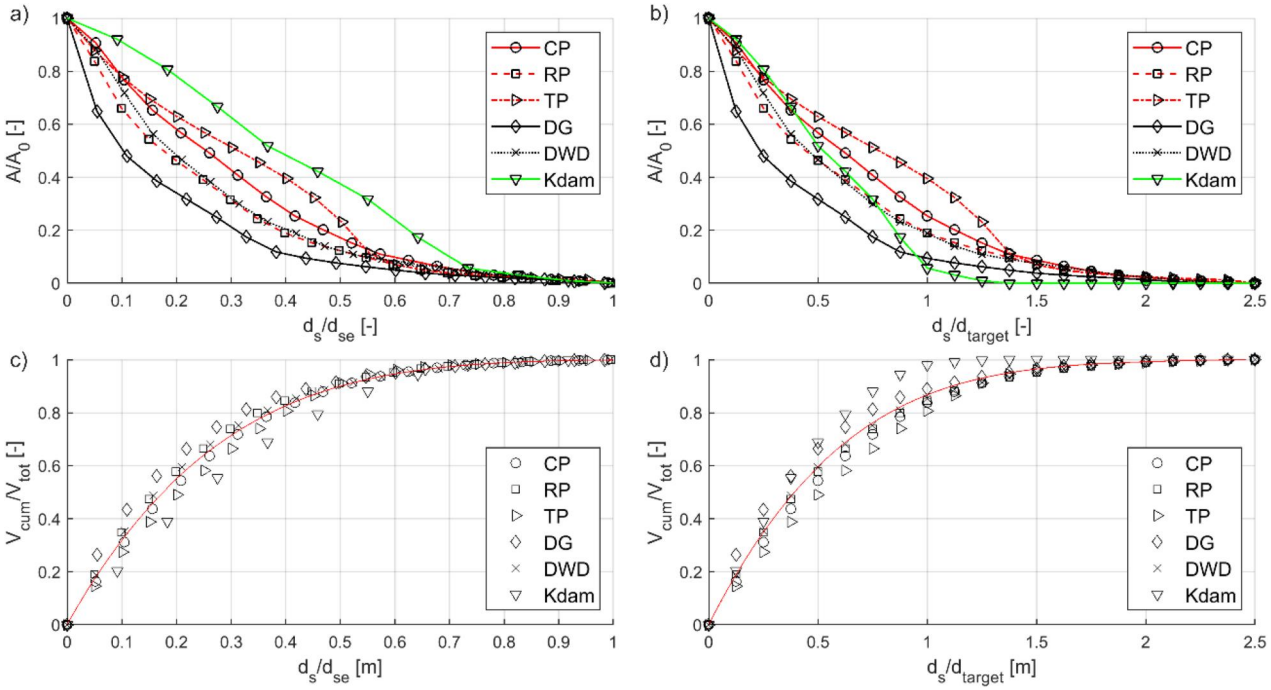

Figure 17. (a) Relative area A/A_0 over relative scour depth d_s/d_{se}, (b) relative area A/A_0 over relative scour depth d_s/d_{target}, (c) relative volume V_{cum}/V_{tot} over relative scour depth d_s/d_{se}, (d) relative volume V_{cum}/V_{tot} over relative scour depth d_s/d_{target}.

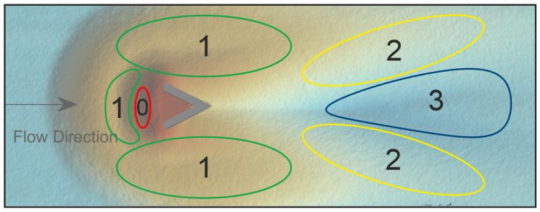

0 - area not suitable as habitat
1 - deep pool habitat (adult habitat)
2 - area with medium flow velocity and a gentle slope (transition zone, adult and juvenil habitat)
3 - gravelbar (spawning area and larvae habitat)

Figure 18. Habitat types in the proximity of a triangular pier (TP) based on bed morphology and visual observations of the flow field.

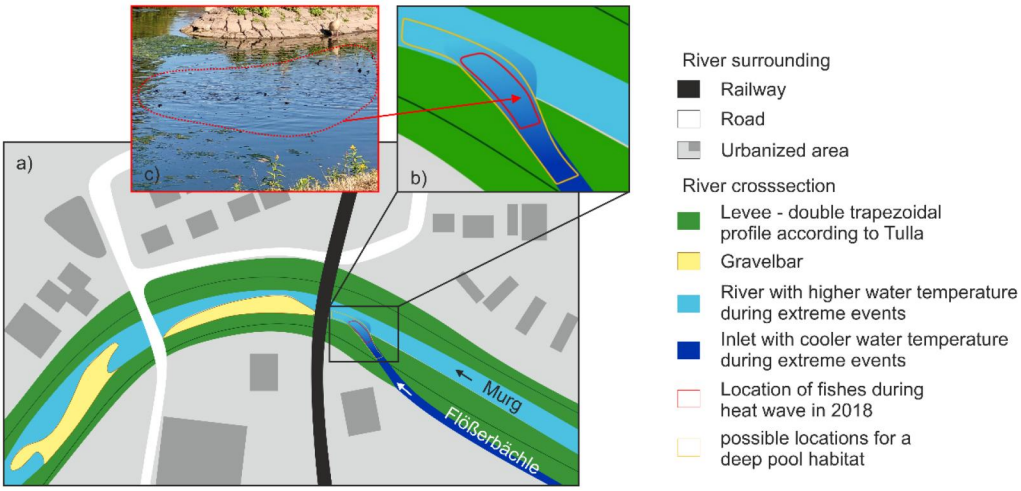

Figure 19. Example of a possible location of a deep pool habitat. a) Location of an inlet of a small creek with cool water temperatures (Flößerbächle) into a bigger river with higher water temperatures (Murg) in an urbanized area. The river lays within two levees in a double trapezoidal cross profile. Downstream of the inlet two big gravelbars are present in the inner bank of the river bend. b) Mixing area of cooler and warmer water. The red frame marks the location where fish looked for a cold-water refugee during the heat wave in 2018 and 2022. The orange frame marks the possible area where a deep pool habitat structure in form of a local scour could be located. c) Accumulation of fishes (see fins) at the cold-water inlet of Flößerbächle during the heatwave 2018 (image courtesy of Dr. Frank Hartmann).

of the deep pool habitat. The importance of incoming tributary valleys for thermal refuges was also reported by Dugdale et al. (2015) in a study on the spatial distribution of thermal refuges. Channel curvature and groundwater thermal refuges (hyporheic upwelling) were identified as other important sites (Dugdale et al. (2015)).

According to observations from statal authorities in the heat waves of the last years, barbels and other fish species accumulated in deep pool habitats where lower water temperatures were present but a lack of systematic investigations is obvious and needs to be performed subsequent to this research. The investigation of appropriate in-stream structures is a large and necessary step towards reaching the goal of creating deep pool habitats. As far as suitable hydromorphological conditions can be provided through the implementation of the in-stream structures, a fishbiological study needs to be performed to investigate whether fish are likely to accept the artificially implemented structures as replacement habitats. Moreover, the aspect of water temperature inside of the deep pool habitat including mixing processes of cold and warm water needs to be further investigated.

7. Conclusion

Clear-water scour experiments have been carried out for six different structures with the intention of creating a deep pool habitat with defined physical parameters: three pier-like structures, two stone-like structures and the Kdam. The scour holes that evolve around the different structures are analysed regarding their characteristics of the scour. All tested structures are able to meet the target values of water depth and area with the pier-like structures creating the deepest and largest scour holes compared to the other structures.

The time development of the scour of pier-like and stone-like structures is characterized by an

asymptotic behaviour, whereas the Kdam shows no asymptotic trend which is attributed to different physical phenomena leading to the scour process. The main processes observed at the structures are a horseshoe-vortex dominated scour, a constriction scour, a shear scour and combinations of the latter.

In equilibrium, all pier-like structures show similar scour pattern with a circular scour hole and the deepest scour position immediately upstream of the pier. Two deep lateral sections reach further downstream and a central dune can be observed. The deepest scour position of stone-like structures is located upstream, at the head of the structure and the scour hole extends upstream and downstream. The dam-like structure creates the deepest scour at the sides of the flume. The experiments show higher sensitivity regarding reproducibility in regions with high slopes, where sliding sediment motion mechanisms were observed, and downstream of the structures. The data shows that the created scour holes qualitatively match very well with the data published in the literature.

The geometrical analysis of the scour holes shows that the necessary area in the target depth can be reached by all structures and that $0.11 - 0.19$ of the total scour volume is located below the target depth of 2 m. Evaluation of the structures regarding their ability to create a habitat shows that all structures can provide a suitable deep pool habitat. The TP stands out with fullfilling more habitat functions as previously intended. Based on habitat suitability parameters water depth, area and volume the TP is therefore the favourable structure for implementation.

Those responsible for river restoration have considerable doubts about in-stream measures, as these could increase the risk of flooding. Since structures have not yet been installed in a "controlled" manner, the hydormorphological structure of river systems are mostly still rudimentary. The backwater rise $\Delta h_1/h_0$ could be characterized in this study and lays in a range of $6.9 - 31.8\%$. Stone-like structures initiate the lowest, pier-like structures an intermediate and dam-like structures the highest backwater rise. The drag coefficients for CP and RP match well with literature values. Therefore, the knowledge gained from this study can reduce this uncertainty in the effect of structures on flood risk. As a result, they are very suitable for being integrated into the planning for the state study on water ecology (LSGÖ). With regard to flood risk management, the Kdam is not suitable for most rivers as it produces a backwater rise of 31.8%. Submerged structures with low blockage area, such as the DG provoke the lowest backwater rise, but also the smallest scour hole.

As a compromise of both habitat suitability and flood risk management the TP is recommended for implementation. It is to be noted that the engineering measures always have to be checked for every location whether they suit the local conditions. This means, e.g. examination of the water surface elevation and height of levees for possible inundations, as well as taking soil samples for a profound foundation of the measures.

The presented measures of the portfolio of in-stream structures can serve as additional instruments to reduce damage to fish stocks caused by climate change. Due to decreasing water depths, rising water temperatures and the associated reduced oxygen content in the water, fish species are under stress. If, in addition, prolonged periods of heat occur, extensive fish kills can occur. These can be reduced or even prevented if there are rest areas for fish with higher water depth and cooler water temperatures. This is achieved through the targeted construction of scours at sources with cool water, such as stream or groundwater inlets. Moreover, through diversification of water depth and flow velocities the overall betadiversity of the river reach can be significantly improved through the presented in-stream structures. Consequently, the benefit of those structures is not exclusively to barbels, but also to other species like macrozoobenthos.

Notation

A_{target}	area in target depth [m²]
A_0	area at the initial bed level [m²]
A_r	blockage ratio [-]
C_d	drag coefficient [-]
D	hydraulically significant length scale $D = w_s * h_s/h_0$ [m]
d_{50}	median diameter [m]
d_s	scour depth [m]
d_{se}	maximum end scour depth in equilibrium stage [m]
Fr_0	approach flow Froude number [-]
Fr_c	critical Froude number [-]
F_d	densimetric Froude number [-]
h_0	approach flow depth without structure (h uniform) [m]
h_1	upstream water depth [m]
h_2	downstream water depth [m]
h_s	height of the structure [m]
$h_{ü}$	overflow height (at sills) [m]
h_d	height of dune [m]
h_v	Energy loss [m]
Δh	h_1-h_2 [m]
g	gravity [m/s²]
K	pier shape factor by Yarnell
l_{dune}	distance of the structure to the highest point of the dune [m]
L	characteristic length [m]
l_s	length of structure [m]
l_{dse}	length of upstream scour hole [m]
t	time [s]
t_e	end time [s]
U_0	approach flow velocity [m/s]
U_c	critical velocity [m/s]
V_s	solid volume [m³]
V_{cum}	cumulated volume [m³]

V_{tot}	total volume [m³]
w	width of the flume [m]
w_s	width of the structure [m]

Greek

ρ	density of water [kg/m³]
ρ_s	density of the sediment [kg/m³]
ν	kinematic viscosity [m²/s]
σ_g	sediment grading or sediment uniformity, $\sigma_g = d_{84}/d_{50}$
ζ	loss coefficient [-]
μ, β	correction factors for the equation of Yarnell
CP	Circular Pier
RP	Rectangular Pier
TP	Triangular Pier
DWD	Double Wing Deflector
DG	Deflected Groyne
Kdam	Kdam
LSGÖ	Landesstudie Gewässerökologie

Disclosure statement

No potential conflict of interest was reported by the authors.

ORCID

Christin Kannen http://orcid.org/0000-0002-0412-4970

References

Addy S, Wilkinson M. 2016. An assessment of engineered log jam structures in response to a flood event in an upland gravel-bed river. Earth Surf Processes Landf. 41(12):1658–1670. doi: 10.1002/esp.3936.

Agisoft Metashape. 2020. Agisoft metashape. In agisoft metashape professional (version 1.6.5) (software). (2020). http://www.agisoft.com/downloads/installer/.

Akhlaghi E, Babarsad MS, Derikvand E, Abedini M. 2020. Assessment the effects of different parameters to rate scour around single piers and pile groups: a review. Arch Comput Methods Eng. 27(1):183–197. doi: 10.1007/s11831-018-09304-w.

Anlauf A, Hentschel B. 2007. Untersuchungen zur Wirkung verschiedener Buhnenformen auf die Lebensräume in Buhnfeldern der Elbe. Wasserstraßen - Verkehrswege Und Lebensraum in Der Kulturlandschaft. Symposium Am; 11 September 2007; Bonn. p. 94–100. https://henry.baw.de/items/a8dab730-bc2f-42b2-9367-d2c19faa0f95.

Armanini A, Sartori F, Tomio G, Cerchia F, Vergnani M. 2010. Analysis of a fluvial groynes system on hydraulic scale model. River Flow. 2010:1177–1184.

Azinfar H, Kells JA. 2008. Backwater prediction due to the blockage caused by a single, submerged spur dike in an open channel. J Hydraul Eng. 134(8):1153–1157. doi: 10.1061/(ASCE)0733-9429(2008)134:8(1153).

Azinfar H, Kells JA. 2009. Flow resistance due to a single spur dike in an open channel. J Hydraulic Res. 47(6):755–763. doi: 10.3826/jhr.2009.3327.

Bănărescu PM, Bogutskaya NG. 2003. In: Bănărescu PM, Bogutskaya NG, editors. The freshwater fishes of Europe, cyprinidae 2, part II: Barbus. Vol. 5. Wiebelsheim, Germany: Aula-Verlag.

Becker A, Ortlepp J. 2022. Landesstudie Gewässerökologie Baden-Württemberg-Fischökologisch funktionsfähige Strukturen in Fließgewässern. Methodik zur Herleitung des strukturellen Defizits als Grundlage der Schaffung von funktionsfähigen Lebensräumen für die Fischfauna in den Gewässern Baden-Württembergs. https://rp.baden-wuerttemberg.de/fileadmin/RP-Internet/Themenportal/Wasser_und_Boden/Geschaeftsstelle_Gewaesseroekologie/Landesstudie_Gewaesseroekologie_G._I._O/_DocumentLibraries/Documents/Fischoekologisch_funktionsfaehige_Strukturen.pdf.

Becker FN, Fink AH, Bissolli P, Pinto JG. 2022. Towards a more comprehensive assessment of the intensity of historical European heat waves (1979–2019). Atmos Sci Lett. 23(11):e1120. doi: 10.1002/asl.1120.

Blohm HP, Gaumert D, Kämmereit M. 1994. Leitfaden für die Wieder- und Neuansiedlung von Fischarten. Binnenfischerei in Niedersachsen. Vol. 3 https://www.laves.niedersachsen.de/startseite/tiere/binnenfischerei/fischartenschutz/-93498.html.

Breusers HNC, Nicollet G, Shen HW. 1977. Local scour around cylindrical piers. J Hydraulic Res. 15(3):211–252. doi: 10.1080/00221687709499645.

Breusers HNC, Raudkivi AJ. 1991. In: Breusers HNC, Raudkivi AJ, editors Scouring (VIII). Cape Town: Balkema.

Britton JR, Pegg J. 2011. Ecology of European barbel Barbus barbus: Implications for river, fishery, and conservation management. Reviews in Fisheries Science. 19(4):321–330. doi: 10.1080/10641262.2011.599886.

Burkow M, Griebel M. 2016. A full three dimensional numerical simulation of the sediment transport and the scouring at a rectangular obstacle. Comput Fluids. 125:1–10. doi: 10.1016/j.compfluid.2015.10.014.

Charbeneau RJ, Holley ER. 2001. Backwater effects of piers in subcritical flow. Texas: University of Texas at Austin. Center for Transportation Research.

Chiew YM, Melville BW. 1987. Local scour around bridge piers. J Hydraulic Res. 25(1):15–26. doi: 10.1080/00221688709499285.

Coleman SE, Lauchlan CS, Melville BW. 2003. Clear-water scour development at bridge abutments. J Hydraulic Res. 41(5):521–531. doi: 10.1080/00221680309499997.

Dey S, Raikar RV. 2007. Characteristics of horseshoe vortex in developing scour holes at piers. J Hydraul Eng. 133(4):399–413. doi: 10.1061/(ASCE)0733-9429(2007)133:4(399).

Dey S, Raikar R. v, Roy A. 2008. Scour at submerged cylindrical obstacles under steady flow. J Hydraul Eng. 134(1):105–109. doi: 10.1061/(ASCE)0733-9429(2008)134:1(105).

Dugdale SJ, Bergeron NE, St-Hilaire A. 2015. Spatial distribution of thermal refuges analysed in relation to riverscape hydromorphology using airborne thermal infrared imagery. Remote Sens. Environ. 160(1):43–55. doi: 10.1016/j.rse.2014.12.021.

El-Alfy KS. 2006. Experimental study of backwater rise due to bridge piers as flow obstructions. 10th International Water Technology Conference; Alexandria, Egypt; Vol. 10. IWTC10 2006; Mar 23-25; p. 319–336.

Euler T, Herget J. 2012. Controls on local scour and deposition induced by obstacles in fluvial environments. Catena. 91:35–46. doi: 10.1016/j.catena.2010.11.002.

Euler T, Herget J, Schlömer O, Benito G. 2017. Hydromorphological processes at submerged solitary boulder obstacles in streams. Catena. 157:250–267. doi: 10.1016/j.catena.2017.05.028.

Fisher A, Klingeman P. 1984. Local scour at fish rocks. In Schreiber D, editor. Water for resource development. Reston (VI); American Society of Civil Engineers; p. 286–290.

Gebhardt M, Pfrommer U, Belzner F, Eisenhauer N. 2012. Backwater effects of Jambor weir sill. J Hydraulic Res. 50(3):344–349. doi: 10.1080/00221686.2012.686712.

Guan D, Liu J, Chiew YM, Zhou Y. 2019. Scour evolution downstream of submerged weirs in clear water scour conditions. Water (Switzerland). 11(9):1746. doi: 10.3390/w11091746.

Guan D, Melville BW, Friedrich H. 2014. Flow Patterns and Turbulence Structures in a Scour Hole Downstream of a Submerged Weir. J Hydraul Eng. 140(1):68–76. doi: 10.1061/(ASCE)HY.1943-7900.0000803.

Harada M, Takaoka H, Oishi T, Kayaba Y, Fujita Y. 2013. Characteristics of bed deformation around submerged groins with various angle. J JSCE. 69(4):I1189–I1194. doi: 10.2208/jscejhe.69.I_1189.

Hentschel B, Henning M, Hüsener T. 2012. Morphologie an buhnenfeldern-nature-und laboruntersuchungen. Wasserbausymposium 2012; Sep 12–15 2012; Graz, Österreich. Munich, Germany: Der TU München, Der ETH Zürich und der TU Graz; p. 403–410. https://hdl.handle.net/20.500.11970/100817.

Huang CC. 1991. Local scour at isolated obstacles on river beds [doctor of philosophy]. Corvallis (OR): Oregon State University.

Ishigaki T, Baba Y. 2004. Local scour induced by 3D flow around attracting and deflecting groins. Second International Conference on Scour and Erosion; ICSE 2, p. 1–8. www.tcpdf.org.

Kalogianni E, Vardakas L, Vourka A, Koutsikos N, Theodoropoulos C, Galia T, Skoulikidis N. 2020. Wood availability and habitat heterogeneity drive spatiotemporal habitat use by riverine cyprinids under flow intermittence. River Res Apps. 36(5):819–827. doi: 10.1002/rra.3601.

Kannen C, Seidel F, Franca MJ. 2022. Discussion of various equilibrium concepts on scouring around hydraulic structures. In: Ferreira da Silva AM, Rennie C, Gaskin S, Lacey J, MacVicar B (Eds.). River Flow 2022 (1st ed.). CRC Press. Kingston and Ottawa, Canada (online). doi: 10.1201/9781003323037.

Khosronejad A, Kang S, Sotiropoulos F. 2012. Experimental and computational investigation of local scour around bridge piers. Adv Water Resour. 37:73–85. doi: 10.1016/j.advwatres.2011.09.013.

Kirkil G, Constantinescu SG, Ettema R. 2008. Coherent structures in the flow field around a circular cylinder with scour hole. J Hydraul Eng. 134(5):572–587. doi: 10.1061/(ASCE)0733-9429(2008)134:5(572).

Kurdistani SM. 2013. Scour downstream of eco-friendly in-stream structures. Pisa, Italy: Università di Pisa Scuola.

LAVES (Hrsg.). 2011. Vollzugshinweise zum Schutz von Fischarten in Niedersachsen. – Fischarten des Anhangs II der FFH-Richtlinie und weitere Fischarten mit Priorität für Erhaltungs- und Entwicklungsmaßnahmen – Barbe (Barbus barbus). – Niedersächsische Strategie zum Arten- und Biotopschutz. http://www.nlwkn.niedersachsen.de/download/50800.

Leibundgut E, Steinbrich H. 2002. Einzugsgebietsbezogene Bewertung der Abfluss- und Stoffdynamik als Grundlage eines Bewertungsverfahrens, Hydrologische Güte "zum operationellen Einsatz im nachhaltigen Flussgebietsmanagement.

Magoulick DD, Kobza RM. 2003. The role of refugia for fishes during drought: a review and synthesis. Freshwater Biol. 48(7):1186–1198. doi: 10.1046/j.1365-2427.2003.01089.x.

Meftah M, Mossa M, Greco M, Carravetta A, Della Morte R. 2004. Experimental study of the scour hole downstream of bed sills. River Flow. 2004:585–592. doi: 10.1201/b16998-76.

Melcher AH, Schmutz S. 2010. The importance of structural features for spawning habitat of nase Chondrostoma nasus (L.) and barbel Barbus barbus (L.) in a pre-Alpine river. River Syst. 19(1):33–42. doi: 10.1127/1868-5749/2010/019-0033.

Melville B. 1997. Pier and abutment scour: integrated approach. J Hydraul Eng. 123(2):125–136. doi: 10.1061/(ASCE)0733-9429(1997)123:2(125).

Melville B. 2008. The physics of local scour at bridge piers. In: Sekiguchi H, editor. Proceedings 4th International Conference on Scour and Erosion (ICSE-4); Tokyo, Japan; Nov 5-7. Japanese Geotechnical Society; p. 28–40.

Melville BW, Chiew YM. 1999. Time scale for local scour at bridge piers. J Hydraul Eng. 125(1):59–65. doi: 10.1061/(ASCE)0733-9429(1999)125:1(59).

Mende M. 2014. Naturnaher uferschutz mit lenkbuhnen–grundlagen, analytik und bemessung [Nature-orientated riverbank protection using micro groynes - principles, analysis and design] [Dissertation]. Braunschweig, Germany: TU Braunschweig.

Morgan JA, Brogan DJ, Nelson PA. 2017. Application of Structure-from-Motion photogrammetry in laboratory flumes. Geomorphology. 276:125–143. doi: 10.1016/j.geomorph.2016.10.021.

Möws R, Koll K. 2014. Influence of a single submerged groyne on the bed morphology and the flow field. In: Schleiss AJ, de Cesare G, Franca MJ, Pfister M, editors. River flow 2014. Boca Raton (FL): CRC Press; p. 1447–1454.

Muhawenimana V, Wilson CAME, Ouro P, Cable J. 2019. Spanwise cylinder wake hydrodynamics and fish behavior. Water Resour Res. 55(11):8569–8582. doi: 10.1029/2018WR024217.

Müller A, Seidel F, Nestmann F. 2020. The effect of micro groins on riverbed structures – Comparison of the velocity distribution in experiments with fixed and mobile bed. River Flow 2020 - Proceedings of the 10th Conference on Fluvial Hydraulics; Delft; 2012; 7-9 Jul. CRC Press; p. 635–643. doi: 10.1201/b22619-90.

Oak AG. 1992. Backwater rise due to a submerged spur [master of science]. Saskatoon, Canada: University of Saskatchewan.

Pagliara S, Hassanabadi L, Kurdistani SM. 2015. Clear water scour downstream of log deflectors in horizontal channels. J Irrig Drain Eng. 141(9):04015007–1–8. doi: 10.1061/(asce)ir.1943-4774.0000869.

Pagliara S, Kurdistani SM. 2013. Scour downstream of cross-vane structures. J Hydro-Environ Res. 7(4):236–242. doi: 10.1016/j.jher.2013.02.002.

Pagliara S, Kurdistani SM, Hassanabadi LS. 2014. Scour characteristics downstream of in-stream river restoration structures: log and J-Hook vanes comparison. In: Lehfeldt K, editor. 11th International Conference on Hydroscience & Engineering - ICHE 2014; September 2014; Hamburg. New York (NY): ICHE; p. 859–864.

Pagliara S, Kurdistani SM, Santucci I. 2013. Scour downstream of J-Hook vanes in straight horizontal channels. Acta Geophys. 61(5):1211–1228. doi: 10.2478/s11600-013-0143-z.

Panchan R, Pinter K, Schmutz S, Unfer G. 2022. Seasonal migration and habitat use of adult barbel (Barbus barbus) and nase (Chondrostoma nasus) along a river stretch of the Austrian Danube River. Environ Biol Fish. 105(11):1601–1616. doi: 10.1007/s10641-022-01352-3.

Peñáz M, Baruš V, Prokeš M, Homolka M. 2002. Movements of barbel, Barbus barbus (Pisces: cyprinidae). Folia Zool. 51(1):55–66.

Pouilly M, Souchon Y. 1994. Physical habitat simulation of barbel (Barbus barbus, L. 1758): Selection of biological models based on predictability criteria. Bull Franc Peche Piscicult. 334:213–225.

Rashak BM, Khassaf SI. 2020. Study the local scour around different shapes of single submerged groyne. J Water Land Dev. 47(1):1–9. doi: 10.24425/jwld.2020.135025.

Raudkivi AJ. 1986. Functional trends of scour at bridge piers. J Hydraul Eng. 112(1):1–13. doi: 10.1061/(ASCE)0733-9429(1986)112:1(1).

Raudkivi AJ, Ettema R. 1983. Clear-water scour at cylindrical piers. J Hydraul Eng. 109(3):338–350. doi: 10.1061/(ASCE)0733-9429(1983)109:3(338).

Roberson JA, Crowe CT. 1993. Engineering fluid mechanics (5th ed.). Boston (MA): Houghton-Miffin.

Schalko I, Lageder C, Schmocker L, Weitbrecht V, Boes RM. 2019. Laboratory flume experiments on the formation of spanwise large wood accumulations: i. Effect on backwater rise. Water Resour Res. 55(6):4854–4870. doi: 10.1029/2018WR024649.

Schalko I, Schmocker L, Weitbrecht V, Boes RM. 2018. Backwater rise due to large wood accumulations. J Hydraul Eng. 144(9):04018056–1-13. doi: 10.1061/(asce)hy.1943-7900.0001501.

Seitz L. 2020. Development of new methods to apply a multiparameter approach-a first step towards the determination of colmation [doctoral thesis]. Stuttgart, Germany: Universität Stuttgart. doi: 10.18419/opus-11249.

Shamloo H. 1997. Hydraulics of simple habitat structures in open channels [doctor of philosophy]. Edmonton, Canada: University of Alberta.

Suribabu CR, Sabarish RM, Narasimhan R, Chandhru AR. 2011. Backwater rise and drag characteristics of bridge piers under sub-critical flow conditions. Eur Water. 36:27–35. https://www.ewra.net/ew/pdf/EW_2011_36_03.pdf.

Thompson DM. 2018. Pool–riffle sequences. Reference module in earth systems and environmental sciences. Amsterdam, Netherlands: Elsevier.

Tritico HM, Cotel AJ. 2010. The effects of turbulent eddies on the stability and critical swimming speed of creek chub (Semotilus atromaculatus). J Exp Biol. 213(Pt 13):2284–2293. doi: 10.1242/jeb.041806.

Umweltbundesamt. 2016. Gewässertypen deutschlands, LAWA-fließgewässertypen, bewirtschaftungskarte: fließgewässertypenkarte. https://gewaesser-bewertung.de/files/typenkarte_fliessgewaesser_bewirtschaftung-skarte_april2016.pdf.

Wang L, Melville BW, Asce M, Whittaker CN, Guan D. 2019. Scour estimation downstream of submerged weirs. J Hydraul Eng. 145(12):06019016–1-7. doi: 10.1061/(ASCE).

Wohl E. 2019. Forgotten legacies: understanding and mitigating historical human alterations of river corridors. Water Resour Res. 55(7):5181–5201. doi: 10.1029/2018WR024433.

Wu S, Rajaratnam N. 1996. Submerged flow regimes of rectangular sharp-crested weirs. J Hydraul Eng. 122(7):412–414. doi: 10.1061/(ASCE)0733-9429(1996)122:7(412).

Yarnell D. 1934. Bridge piers as channel obstructions. http://ageconsearch.umn.edu.